

WATER MASSES AND CIRCULATION
OF THE MOZAMBIQUE CHANNEL

BY

ROALD SÆTRE
INSTITUTE OF MARINE RESEARCH
BERGEN - NORWAY

AND

ANTÓNIO JORGE DA SILVA
INSTITUTO DE DESENVOLVIMENTO PESQUEIRO
MAPUTO - MOZAMBIQUE

NOVEMBER 1982

CONTENTS

	Page
INTRODUCTION	5
MATERIALS AND METHODS	6
WIND CONDITIONS	9
FRESHWATER RUNOFF	11
WATER MASSES AND THEIR SOURCES	14
Previous classification	14
Water structure of the Mozambique Channel	19
Distribution and propagation of water masses	21
Water masses along the Mozambique coast	25
CIRCULATION	31
Circulation pattern along the Mozambique coast	31
General feature in the Mozambique Channel	34
CONCLUSION	36
REFERENCES	37
TABLES	43
FIGURES	49

INTRODUCTION

The Mozambique Current is usually considered as a part of the anti-cyclonic sub-tropical gyre consisting of the South Equatorial Current, the Agulhas Current system and the eastward flow situated to the north of the sub-tropical convergence (Figure 1). The classical concept of the Agulhas Current being an extension of the Mozambique Current has been questioned by MENACHÉ (1963). He claimed that during October-November 1957 the water transported by this current turned back at the southern mouth of the Mozambique Channel and flowed north along the west coast of Madagascar. Due to poor coverage in some key areas, the data of MENACHÉ (1963) may, indeed, be interpreted in a way which allows for outflow from the Mozambique Channel. However, his interpretation has been partly confirmed by HARRIS (1972) during August-September 1964. LUTJEHARMS (1976), making use of all the available data from the north-east monsoon season, concluded that the origin of the inflow to the Agulhas Current is a function of depth and that the Mozambique Current is the major source for the upper water layers during this season.

By isentropic analysis of the quasi-synoptic data from 1964 HARRIS (1972) showed the presence of a front of contrasting water properties along the eastern boundary of the Mozambique Current. Along this front a series of deep anti-cyclonic vortices were identified. The front is probably subject to short-term variability. PEARCE (1977) shows meandering over tens of kilometers in the Agulhas Current off Durban. The time and length scales of these seem to be 4 to 6 days and 200 km respectively.

The northern part of the Mozambique Current as well as its main source, the South Equatorial Current, is directly influenced by the monsoon winds. Considerable seasonal variations in velocity and volume transport are therefore to be expected. The South Equatorial Current is strengthened during the south-west monsoon in April-October. According to WYRTKI (1973) only one third of the South Equatorial Current water turns south as the East

Madagascar and the Mozambique Current. It is likely, however, that this ratio is also subject to seasonal variations. There are significant discrepancies in the available information on the seasonal variations of the Mozambique and Agulhas Current (LUTJEHARMS, 1977, GRÜNDLINGH 1980). In addition to seasonal variations, the interannual variability also seems to be significant (LUTJEHARMS, 1972).

Originally, the present authors' main concerns were the circulation pattern and water mass distribution in the upper 500 m of the waters off Mozambique. However, the nomenclature used on the water masses and water structure of the south-western Indian Ocean and in the Mozambique Channel lacks uniformity. The main reason for the discrepancies is the disagreement on the place of origin as well as on the route of propagation for some of the water masses. Additionally, the circulation pattern along the coast of Mozambique only reflects that of the Mozambique Channel. Therefore, data covering the whole Mozambique Channel were included in this publication in an attempt to clarify these matters. Data on freshwater runoff and wind from the Mozambican coast are presented as these are regarded as necessary background information.

MATERIALS AND METHODS

During the period 1977 to 1980 several research cruises were carried out in Mozambican coastal waters, during which oceanographic data were collected. The distribution of hydrographic and bathythermograph stations by time and sub-areas appears in Table 1. The stations situated on the shelf of Sofala Bank (Area C) and in Delagoa Bay (Area E) have not been included, as the shelf processes were considered outside the scope of this presentation. Figure 2 shows the distribution of the hydrographic and bathythermograph stations carried out during the period, as well as the splitting into sub-areas. The lines dividing the Mozambican coast into sub-areas, were drawn approximately perpendicular to the depth contours giving five areas of different hydrographic characteristics. Table 2 shows the previous cruises

in the Mozambique Channel from which data have been used. The bathymetric conditions of the Mozambique Channel are shown in Figure 3.

The following research vessels participated in these investigations: DR. FRIDTJOF NANSEN from Norway, NIKOLAY RESHETNYAK and MYSLITEL from the Soviet Union, and ERNST HAECKEL and ALEXANDER VON HUMBOLDT from the German Democratic Republic. The main objectives of these cruises were investigations into different aspects of the fishing potentials of the area, except the ALEXANDER VON HUMBOLDT cruise which was devoted to biological, chemical and physical oceanography only.

The data from DR. FRIDTJOF NANSEN have been presented by SÆTRE and PAULA E SILVA (1979) and BRINCA, REY, SILVA and SÆTRE (1981) and those of ERNST HAECKEL by JORGE DA SILVA, MUBANGO and SÆTRE (1981). The results from the ALEXANDER VON HUMBOLDT cruise are presented in ANON (1981). Internal cruise reports have been made presenting the observations from NIKOLAY RESHETNYAK and MYSLITEL.

The hydrographic observations were carried out by Nansen haul, except on the ALEXANDER VON HUMBOLDT which used a CTD system equipped with an oxygen sensor. Samples were taken at the following depths: 0-10-20-30-(40)-50-75-100-(125)-150-200-300-400-500 m. ERNST HAECKEL sampled at 40 m instead of 50 m and 125 m was only sampled by DR. FRIDTJOF NANSEN. In March 1979 ERNST HAECKEL observed down to 1200 m, but only to 600 m in 1980. Nutrients were not investigated by DR. FRIDTJOF NANSEN and MYSLITEL. Usually, unprotected thermometers for depth indication were used, except on DR. FRIDTJOF NANSEN and ERNST HAECKEL in 1980. During all cruises, except that of ERNST HAECKEL in 1979, bathythermographs were used down to 200 or 250 m. The bathystations also included samples of surface salinity. The salinities were obtained by bench salinometers and calculated according to the UNESCO tables of 1966.

Wind data have been supplied by the Meteorological Service of Mozambique and data on the freshwater runoff by the National Directorate for Waters in Maputo.

All the data have been scrutinized and obviously wrong observations deleted. In relation to the salinity values, the high consistency between the different cruises indicates an acceptable quality of data. The oxygen values from some cruises, however, show a suspiciously high scattering (Figure 27), which is most likely due to bad sampling.

Figure 4 shows a $t-\sigma_t$ scattering diagram containing all observations off Mozambique appearing in Table 1. As can be seen, there is a close and near-linear relationship with a change in the slope at about 16°C , i.e. at the subsurface salinity maximum. Table 3 gives the linear regression coefficients for the hydrographic data from DR. FRIDTJOF NANSEN in 1977 and 1978. These data were chosen as they represent a homogeneous data base and are scattered along the whole coast as well as throughout the year. As can be seen from Table 3, there are very strict relationships between σ_t and temperature when salinities below $35^{\circ}/\text{oo}$ in the surface layer are deleted. This means that the interior mass distribution is fairly well described by the temperature field.

To obtain a picture of the circulation pattern with some quantitative meaning using a horizontal temperature distribution, a depth of at least 300 m should be used in order to avoid the region of change in the slope of the $t-\sigma_t$ relationship. This depth is, however, not attainable by bathythermographs. A depth of 150 m was than chosen for purely qualitative purpose.

By using the bathystations a better spatial resolution for the circulation pattern can be reached. For the ALEXANDER VON HUMBOLDT cruise the temperature readings from the CTD sonde were used.

The water structure distribution was mapped by grouping the hydrographic stations covering the whole Mozambique Channel according to the pattern of their $t-S$ diagram. The distribution and way of propagation of the different water masses were mapped by the core method. The core layers considered, appear in Figure 5

The dynamic topography of the surface relative to the 500 decibar level from the six cruises referred to in Table 2 was used in order to obtain an idea of the general circulation in the whole Mozambique Channel.

By dealing with such open grids of stations, e.g. Figure 18, the process of contouring involves subjectivity and one tends to put an element of interpretation into it. The results both on the distribution on core layer and the dynamic topography should therefore be treated with caution, and the distributions regarded as one of several possibilities of interpretation.

WIND CONDITIONS

According to TINLEY (1971) northern Mozambique is affected by the southern extension of the East African Monsoon System with winds blowing from north to north-east during the southern summer and from south to south-west during the southern winter. Central and southern Mozambique is affected by the South-east Trade Wind System and receives easterly prevailing winds throughout the year. According to RAMAGE (1969) the monsoon system influences the Mozambique Channel to latitudes 17° - 18° S. This is also the region of highest incidence of tropical cyclones which occur during the north-east monsoon season, from November to April (TINLEY, 1971).

In order to select some stations that could be taken as representative for the situation at sea, information on wind direction and force collected during the research cruises in 1977-1980 was compared with data from the coastal meteorological stations. The locations of these appear in Figure 6. Data from the meteorological stations at Pemba, Quelimane, Vilanculos and Maputo show appreciable agreement with wind direction at sea while the wind force tended to be higher at sea. Table 4 presents tentative factors for converting wind force ashore to wind force at sea.

Although data from only four coastal stations have been presented, data from all stations have been analyzed. This analysis

revealed that the monsoon system extends along the Mozambique coast only to latitude 15°S . Data from Mocímboa da Praia, Pemba and Lumbo (Figure 6) showed excellent consistency. Therefore, only one station, Pemba, is used to describe the wind regime in the region affected by the monsoon system.

Figure 7 shows, on a monthly basis, 10-year average distributions of wind frequencies and forces per direction for the selected meteorological stations. At each station observations were made at 0900, 1500 and 2100 hours. The picture shown in Figure 7 fits well the description of TINLEY (1971). In the northern region wind prevails from north-east during October-February and from south-east to south during April-September. The strongest winds are associated with the south-west monsoon season. In the central and southern regions the prevailing winds are easterlies, with southerlies becoming important between May and July. Strongest winds are easterlies at Quelimane and southerlies at Vilanculos. At the extreme south, Maputo, the situation is somewhat unclear due to a wide wind spectrum and similar average wind forces regardless of direction. No study has been made by the present authors concerning extreme wind forces, but according to TINLEY (1971) winds of gale force are most frequent south of latitude 15°S .

The all-day situation depicted in Figure 7 shows a rather blurred picture for some of the stations. This is due to diurnal variation in wind direction, with nocturnal offshore winds and onshore winds during daytime. According to TINLEY (1971), the nocturnal land breeze occurs all over the coast, with particular incidence in midwinter mornings, and is a marked feature of at least the central region during both winter and summer months.

Figure 8 shows the wind frequency per direction at 1500 hours in central and southern Mozambique during 1978, 1979 and 1980. The diurnal sea breeze associated with the easterly anti-cyclone (TINLEY, 1971) comes out quite clearly in this figure. Inter-annual variations can also be seen, such as the southerly shift of the wind pattern at Quelimane in 1980 and the presence of a strong southerly component at Vilanculos in 1978.

The nocturnal land breeze does not seem to be as important in the northern region as it is in the central and southern regions, judging by the situations depicted in Figure 9. This figure reveals, however, an important aspect concerning inter-annual variations. The north-east monsoon seasons in 1978, 1979 and 1980 were characterized by easterly prevailing winds, instead of northeasterly as shown in Figure 7. This situation, contrasting with the situations for all other previous years since 1968, was confirmed by wind data from the other stations in the northern region. Variations in the beginning of the north-east monsoon season also come out clearly from Figure 9. The south-west monsoon season, however, did not show any significant variations during these three years.

FRESHWATER RUNOFF

Figure 6 shows the main rivers of Mozambique together with a rough estimate of the average annual runoff in km^3 for the period 1960-1975 (1960-1974 for the Zambezi, 1970-1980 for the Limpopo), split into three regions. No estimate is given for the runoff of the Rovuma river due to lack of information. This river is, however, believed not to contribute significantly to Mozambican waters. Less important rivers in central and southern Mozambique have also been included in Figure 6 because altogether their freshwater contributions cannot be neglected.

An average annual freshwater runoff of about 141 km^3 has been worked out, 85% entering the sea in the central region. The Zambezi alone contributes 67% of the total for all the rivers (the Rovuma excluded). All these rivers carry large amounts of silt, and sandbanks occur far out to sea in the central region (TINLEY, 1971). Minor rivers (less than $0.4 \text{ km}^3/\text{year}$) have not been included in these calculations, their overall contribution having been merely "guesstimated". On the other hand, the runoff values at the runoff gauge stations (Figure 6) have been taken for the total values at the river mouths. This will, of course, lead to some underestimation, particularly for the Zambezi, where the stations were quite far upstream.

ATAIDE (1981) presented estimates of the total freshwater runoff at the river mouths of Mozambique. To do this estimate, specific runoff values at the available stations have been used, and the downstream contributions were assumed to be the same as those upstream of the stations (ATAIDE, personal communication).

This procedure will lead to an overestimation of the freshwater contribution, particularly in the main international rivers, e.g. the Zambezi. The authors' and ATAIDE's (1981) values are compared in Table 5. The Rovuma runoff was estimated using the specific runoff for the area and the total area of the Rovuma basin (ATAIDE, personal communication).

ATAIDE (1981) claims that his figure of 162.8 km³ represents roughly 89% of the freshwater runoff in Mozambique, which gives approximately 180 km³ as the total value. If the Rovuma runoff is subtracted from this value one would be left with 167 km³ to be compared with 141 km³, as found by the present authors. The average annual runoff will probably be somewhat between these values and a preliminary figure of 150 km³ can be taken to represent the mean annual freshwater volume entering the ocean waters of Mozambique.

Variations

The freshwater runoff is clearly seasonal, most of the rivers discharging 60-90% of the total for the whole year between January and April (Table 6). Figure 10 shows the distributions of the average monthly runoff and the variability coefficients, C_v , for the main rivers.

$$C_v = \frac{s}{\bar{Q}} \cdot 100\%$$

where \bar{Q} is the average monthly runoff and s is the standard deviation. Additionally, the variability coefficients for the average yearly runoff are also presented. Generally, all the rivers show a maximum outflow in February-March and a minimum in October (SÆTRE and PAULA E SILVA, 1979). Although the flood

peaks tend to occur during the same months in all rivers, the extension of the flood season may vary, as can be seen in Table 6. The fluctuations are high, with the monthly variability coefficients usually higher than annual variability coefficients. This suggests interannual displacements of the beginning and duration of the flood season, which is confirmed by the occurrence of a maximum value of C_v in November-December for most of the rivers.

The intensity of the seasonal trend also differs from one river to another, being lowest in the Incomati and the Maputo rivers and highest in the Save (Table 6 and Figure 10). The low seasonality of Incomati and Maputo rivers, is due to the frequent and somewhat irregular occurrence of two flood peaks with two to four months difference.

Table 7 shows the average, highest and lowest annual runoff values for some of the main rivers of Mozambique. As seen in Figure 10, the variability coefficient for the annual outflow is highest in the Save river with a value of more than 100% and lowest in the Zambezi with 35%.

Some further comments on the Zambezi are thought to be necessary. First of all, runoff values refer to Tete, a town situated quite far inland, and two important affluents occur downstream of this (Figure 6): Luenha (annual runoff of 5.2 km^3 , on a 6-year average) and Chire (annual average value for 1942-1964: 10.0 km^3). Due to little overlapping between the averaging periods for the Zambezi, the Luenha and the Chire it was impossible to show the seasonal and interannual trends of the Zambezi with all the main contributions. The annual average runoff values shown in Figure 10 for the Zambezi are thus underestimated by approximately 16%. However, the seasonal trend will be quite close to that shown in Figure 10 because the affluentes fit the Zambezi trend. In fact, the Chire shows very little seasonality but, on a monthly basis, its contribution is not enough to introduce major changes to the Zambezi runoff.

Since 1958 the Zambezi regime has been controlled by the Kariba dam in Zimbabwe and thus all the available data until 1974 reveal a regime which most likely is different from the natural one. Late in 1974 another dam was put into operation at Cahora-Bassa, approximately 200 km upstream of Tete. Figure 11 clearly shows that the operation of this dam introduced drastic changes in the seasonal pattern of the Zambezi runoff.

WATER MASSES AND THEIR SOURCES

Previous classification

Several authors have tried to characterize the different regions of the Indian Ocean according to the water structure. Figure 12 shows the classifications north of the subtropical convergence applied in some of the main works. The classification of SVERDRUP et al. (1942) was based on the different origins of the sub-surface water masses usually found between 200 and 600 m. IVANENKOV and GUBIN (1960) apparently used the distribution of surface water for their division of zones.

SHCHERBININ (1969) deals with the equatorial Indian Ocean only, which he splits into three different structures. The three structural types are separated by two fronts extending zonally.

The classification of KUKSA (1972), however, is based on the horizontal extent of intermediate layers, which he claims is essentially equivalent to the distribution of water structure types. He introduces a West Madagascar variety of the South Tropical structure. This variety differs from the main structure in absolute values of temperature and salinity while the t-S pattern is basically the same. In a later work, BURKOV and KUKSA (1977) present another classification which is also apparently based on the same criterion.

A different approach is taken by WYRTKI (1973). On a large scale he distinguishes between three circulation systems in the Indian Ocean:

- a) the seasonally changing monsoon gyre,
- b) the sub-tropical anti-cyclonic gyre,
- c) the Antarctic waters.

The monsoon gyre is separated from the southern sub-tropical gyre by a pronounced hydrochemical front at about 10°S . The present authors consider this as the most fruitful classification.

Figure 13 shows some idealized t-S curves from two hydrographic sections across the northern (between $10^{\circ}40'\text{S}$ and $12^{\circ}40'\text{S}$) and southern (approximately along 26°S) parts of the Mozambique Channel. The data are from the cruises of ATLANTIS II in 1963 and 1965 and elucidate the typical t-S distributions observed in the area. As can be seen, the water column has been split into five zones, each containing one or more water masses. The divergence in terminology of the water masses in the upper four zones appears in Table 8.

Surface water

In the Mozambique Channel this zone is considered as the upper 100-150 m. It is usually believed to consist of two different water masses separated by a transition area between 22°S and 27°S . The northernmost warm low-salinity surface water is considered to be brought into the area by the South Equatorial Current, while the southernmost originates from that formed in the center of the sub-tropical anti-cyclonic gyre of the Indian Ocean.

IVANENKOV and GUBIN (1960) introduce the terms South Equatorial and Tropical water for the northernmost and southernmost surface waters respectively. They also use the term Sub-tropical surface water, but only for water between the sub-tropical convergence and about 34°S .

MAGNIER and PITON (1973) and PITON, POINTEAU and NGOUMBI (1981) follow the surface water classification of IVANENKOV and GUBIN (1960). They state, however, that the surface water between 12°S and 22°S inside the Mozambique Channel has a closed anti-cyclonic circulation and is influenced mainly by the local seasonal variations. For that reason they term this water South Equatorial Mozambique Channel water.

Most other authors, mainly South Africans, dealing with the water mass distribution in the area, use the terms Tropical and Sub-tropical water. The name Agulhas water was originally introduced by J. DARBYSHIRE (1964) based solely on temperature. M. DARBYSHIRE (1966) uses the same term for the warm and low-salinity water of tropical origin which is closely related to the Agulhas Current. What she refers to as Boundary water represents conditions somewhere between those of the Agulhas and the extreme Sub-tropical water.

Sub-surface water

This term is applied to the water characterized by a salinity maximum found in the Mozambique Channel at depths between 150 and 300 m (Figure 13). The different terminology used for this water mass appears in Table 8.

The main reason for this diversity in terminology seems to be the uncertainty as to whether the salinity maximum in the central and northern part of the Mozambique Channel is caused by water coming from the north or from the south. According to WYRTKI (1971) two water masses form what he calls "the shallow salinity maximum" of the Indian Ocean: the Sub-tropical Surface water of the southern sub-tropical gyre, and the Arabian Sea Surface water. Both are propagating equator-ward and meet near 10°S.

KHIMITSA (1968), following the classification of IVANENKOV and GUBIN (1960) for the Indian Ocean, presupposes a southward propagation of what he calls the South Equatorial Sub-surface

water. According to IVANENKOV and GUBIN (1960) this water is formed in the region of the south equatorial divergence between 8°S and 12°S by Tropical Surface water and the rising Sub-tropical Sub-surface water.

MAGNIER and PITON (1973) believe in a southward penetration into the Mozambique Channel of high-salinity water of Arabian origin at a depth of about 200 m, for which they have some support from the work of ROCHFORD (1964). They name this water North Equatorial water of the northern Mozambique Channel. Tropical water is found in the southern part of the Channel, and these two water masses are separated by a transition zone.

ISAENKO et al. (1980) follow the same scheme though they attribute different names to the water masses. MAGNIER and PITON (1974), however, indicate the possibility of high-salinity water from the south rounding the northern tip of Madagascar into the Mozambique Channel.

Central water

SVERDRUP et al. (1942) introduced the term Indian Ocean Central water for the water mass lying approximately in the depth range 300 to 600 m. This water is characterized by a near-linear t-S relationship between the points (8°C , $34.6^{\circ}/\text{oo}$) and (15°C , $35.6^{\circ}/\text{oo}$). North of about 10°S SVERDRUP et al. (1942) use the name Equatorial water for that linear part of the t-S curve connecting the points (4°C , $34.9^{\circ}/\text{oo}$) and (17°C , $35.25^{\circ}/\text{oo}$). According to LUTJEHARMS (1971) both these water masses are present in the Mozambique Channel.

MUROMTSEV (1950) used the name Sub-tropical Sub-surface water for the Central water mass. This expression has been adopted by several later Soviet authors, as can be seen in Table 8. BURKOV and KUKSA (1977) call it the Main Pycnocline water. Among western scientists the name Central water seems to be generally accepted (Table 8).

SVERDRUP et al. (1942) consider the Central water to originate from the sinking of mixed water just north of the sub-tropical convergence with a subsequent northward spreading. This concept is supported by IVANENKOV and GUBIN (1960), WYRTKI (1971) and BURKOV and KUKSA (1977). CLOWES (1950), however, claims this water to be the result of vertical mixing between the Sub-surface and Intermediate water while ORREN (1963) believes more in a combination of these two postulations.

Intermediate waters

There is two types of intermediate waters present in the Mozambique Channel; the low-salinity water of Antarctic origin and the high-salinity water originating from the Northern Indian Ocean. Most of the authors have accepted the term Antarctic Intermediate water for the low-salinity water formed at 50^o-55^oS. IVANENKOV and GUBIN (1960), however, called it Sub-antarctic Intermediate water.

The high salinity water is formed in the Arabian Sea with the contribution of waters from the Red Sea and the Gulf of Oman. PITON, POINTEAU and NGOUMBI (1981) consider an upper and lower Antarctic Intermediate water separated by Red Sea water.

Deep and bottom water

The salinity maximum usually found at depths of 2700-3200 m in the southern part of the Mozambique Channel (Figure 13), is caused by an intrusion of North Atlantic Deep water (CLOWES and DEACON, 1937). This water is probably forced back to the south by the shallow depths of the Mozambique Channel (LE PICHON, 1960). This is also the case for the Antarctic Bottom water. PITON, POINTEAU and NGOUMBI (1981), however, consider the North Atlantic Deep water to occupy all the deeper layers of the Mozambique Channel. The deep and bottom water will not be further considered in this presentation.

The present authors will adopt the following terminology for the different water masses of the Mozambique Channel for which arguments will be presented later:

Equatorial Surface water, Sub-tropical water, Central water, Antarctic Intermediate water and North Indian Intermediate water.

The Sub-tropical water can be found both at surface and at subsurface levels.

Water structure of the Mozambique Channel

The t-S curves for each hydrographic station from the six cruises covering the whole Mozambique Channel (Table 2) were grouped into three different categories according to the t-S pattern shown in Figure 14. Scattering diagrams for the different structures appear in Figures 15 and 16. $\frac{A}{B}$ is a transition structure, where the layer down to the upper part of the Central water is of A type and the lower layer of B type. The structures $\frac{B}{A}$, $\frac{C}{B}$ and $\frac{B}{C}$ are defined in a similar way. The difference between A and $\frac{A}{B}$ structure can be seen in Figure 17a.

Structure A

This structure is characteristic for the area south of approximately 25°S. A slight salinity maximum indicates the Sub-tropical water at about 17°-18°C. The quasi-linear slope from 15° to 8°C marks the Central water and the salinity minimum at about 5°C the Antarctic Intermediate water. Another salinity maximum occurs at about 2°C caused by the presence of North Atlantic Deep water.

Structure B

This structure is observed in the central part of the Mozambique Channel. The salinity maximum of the Sub-tropical water is reduced and occurs at 15°-17°C. The slope of the Central water

has increased compared to structure A, and the salinity minimum due to the influence of the Antarctic Intermediate water at 7°-8° is reduced. The slight salinity maximum at about 5°C indicates the presence of the North Indian Intermediate water.

Structure C

This structure is usually found off the East African coast north of 10°S. The data in Figure 16 are from the cruise of COMMANDANT ROBERT GIRAUD in July-August 1960 from 7°-10°S. The salinity decreases with depth to a slight salinity minimum at 9°-10°C. There is a salinity maximum due to the North Indian Intermediate water at about 7°C. This maximum is very pronounced in the single t-S diagram, but as its corresponding temperature varies the maximum appears less marked in the scattering diagram. Though this water structure has not been observed in the Mozambique Channel, transitions between structures B and C are occasionally found and for that reason the C structure has been included.

In the t-O₂ diagram there is also a pronounced difference in the A and B structures as can be seen in Figure 17b. The A structure has a higher oxygen content than that of B except for temperatures below 4°C. We suggest the following names for the water structures: A) Sub-tropical structure, B) Mozambique Channel structure, C) Western Equatorial structure.

Figure 18 shows the distribution of water mass structures from the six cruises which covered more or less the whole Mozambique Channel. As can be seen, most of the Channel is characterized by the B structure. In the southern part there is a transition zone of mainly $\frac{A}{B}$ structure. At two stations off Maputo from the ALMIRANTE LACERDA's cruise in April-May 1964 a water structure was observed which was neither A nor B. It might be explained by an intense mixing in this area due to eddy formation. The borderlines between the A and B structures in the upper and lower layers give some indications of the outflow from the Mozambique Channel, which is illustrated by arrows.

Distribution and propagation of water masses

In the lower layer the southerly outflow is mainly due to North Indian Intermediate water, as can be seen in Figure 19, showing properties along the intermediate salinity maximum. This water, found at depths of 700-1500 m, enters the Mozambique Channel along the coast of Mozambique and leaves it on the eastern side. The intermediate salinity maximum associated with this outflow has not been observed on the western coast south of 22° to 25° S.

The southerly outflow in the upper layer seemed to be completely blocked during the cruises of COMMANDANT ROBERT GIRAUD in 1962 and ALMIRANTE LACERDA September-October 1964 (Figure 18).

HARRIS (1972), by using the ALMIRANTE LACERDA data, concludes that during that cruise an outflow occurred. However, this seems to be more a recirculation at about 25° S rather than a southward propagation of water from the Mozambique Channel. Indication of an outflow along the Mozambican coast was found during the cruises of COMMANDANT ROBERT GIRAUD in 1957 and 1960 and ALMIRANTE LACERDA in April-May 1964. During the cruise of ALIDADE in 1952 the outflow was apparently confined to an offshore narrow band separated from the coast by a northward intrusion of water of A-structure.

The salinity minimum due to the Antarctic Intermediate water as seen in the A structure, seems to be rather homogeneous over a huge area in the south-western Indian Ocean (e.g. ORREN, 1963). In the transition zone in the southern part of the Mozambique Channel there is an abrupt change due to mixing with the North Indian Intermediate water. The salinity values in the minimum layer are increased by approximately $0.2^{\circ}/\text{oo}$ and the horizontal salinity gradient reaches a maximum within the transition zone as can be seen in Figures 20a and d.

Figures 20b and c, showing typical examples of the topography of the Intermediate salinity minimum, indicate an anti-cyclonic circulation with a southward curving of the Antarctic Intermediate water. The position of this curve seems to vary between

20° and 25°S, i. e. the same latitude range where the North Indian Intermediate water turns southeastwards. Though most of Antarctic Intermediate water seems to recirculate within the Channel, a minor part of it probably penetrates further north. It is not clear if this water really passes through the Mozambique Channel.

The data on the salinity distribution in the core of the Antarctic intermediate water from the COMMANDANT ROBERT GIRAUD cruise of 1962 (Figure 20d) indicates that this water sometimes might round the northern tip of Madagascar and intrude into the Mozambique Channel from the north. The same feature can be seen in the distribution of temperature and salinity at the core layer of the Antarctic Intermediate water in the atlas of WYRTKI (1971).

The other source of low-salinity intermediate water in the Indian Ocean is the Banda Intermediate water. According to ROCHFORD (1966) this can penetrate as far as the Northern Mozambique Channel. DONGUY and PITON (1969) claim this water to be present at a fixed hydrographic station off the north-western coast of Madagascar at depths between 1400 and 1900 m. If this water, of $\sigma_t > 27.6$, really intrudes into the Mozambique Channel it must be below the North Indian Intermediate water. However, no indications of such an intrusion can be seen in the present data.

The northbound Sub-tropical water seems to have an anti-cyclonic circulation according to the topography and salinity distribution at the sub-surface salinity maximum from the ALIDADE 1952 and COMMANDANT ROBERT GIRAUD 1957 data (Figures 21a-d). The sub-tropical water penetrates the Mozambique Channel on its eastern side and turns westward at about 18°S. Also, during the other cruises, the northward flow on the eastern side of the channel was pronounced (Figures 21e and f, 22) while the apparent anti-cyclonic circulation centered at about 18°-20°S was not clearly seen due to poor data coverage in the actual area. However, hydrographic sections across the channel along the 20°S parallel

always show the characteristic feature of an eddy with a splitting of the sub-surface salinity maximum into two separate parts (e.g. Figure 23). A third salinity core is present also at the eastern part of the Channel associated with a southerly current. The apparent eddy with a recurving of the Sub-tropical water can be seen in the isentropic analysis of LUTJEHARMS (1976) from November to April, and in that of HARRIS (1972) from August-September 1964. As for the Antarctic Intermediate water a minor part of the Sub-tropical water seems to penetrate further north along the coast of Madagascar.

There are also some slight indications of subsurface penetration of high salinity water into the Mozambique Channel from the north. This can be seen from the data of the COMMANDANT ROBERT GIRAUD cruises of 1960 and 1962 (Figures 21e and f) where an area of high salinity water was observed off the northern tip of Madagascar. This water seemed to have an anti-cyclonic circulation in the northern part of the Channel. The same pattern was also observed by HARRIS (1972). DONGUY and PITON (1969) concluded that during the time of the north-east monsoon an anti-cyclonic eddy seemed to be established around the Comores, while during the south-west monsoon season water entered this area from further south of the Mozambique Channel. MAGNIER and PITON (1974) by dealing with data from the north-east monsoon season, found that both Sub-tropical water and Central water was coming from eastern Madagascar into the northern part of the Mozambique Channel. The present data do not show any evident contribution of high-salinity water of Arabian Sea origin entering the Mozambique Channel at sub-surface level.

The surface water of the Mozambique Channel is mainly made up of Equatorial Surface water coming from the north and Sub-tropical water entering from the south. These water masses are modified within the Channel by vertical and horizontal mixing, as well as by evaporation, precipitation and freshwater run-off. The average natural freshwater run-off in the western area has a maximum in February-March and a minimum during the period September-November (Figure 10). The water transported by the South Equatorial

Current into the Mozambique Channel shows its lowest salinity during March-April and its highest during November-December (DONGUY and PITON, 1969, WYRTKI, 1971, DONGUY, 1975).

Figure 24 shows two surface salinity distributions. Usually, the highest salinities are found along the eastern part of the Channel. Sometimes there seems to be water of equatorial origin rounding the southern part of Madagascar e.g. during the COMMANDANT ROBERT GIRAUD cruise of 1962 (Figure 24).

The water of sub-tropical origin seems to follow two routes; one is forming part of the anti-cyclonic circulation at about 20°S previously mentioned for the sub-surface salinity maximum, while the other propagates further north along the eastern side of the Channel close to Madagascar. The same pattern can also be seen by the surface salinity distribution observed on the COMMANDANT ROBERT GIRAUD in 1957 (MENACHÉ, 1963). In addition to these northward routes there seems in some cases to be a southward penetration of low-salinity water from the north between the two northward routes, e.g. during the COMMANDANT ROBERT GIRAUD cruise of 1962 (Figure 24). The hydrographic section along 20°S from this cruise (Figure 23a) shows water of salinity less than 35.1‰, with the core at about 50 m, which seems to be propagating southwards.

Based on the above analysis, the present authors suggest the following terminology of the water masses of the Mozambique Channel:

- North Indian Intermediate water
- Antarctic Intermediate water
- Central water
- Sub-tropical water
- Equatorial Surface water.

North Indian Intermediate water is preferred as it is in accordance with the term Antarctic Intermediate water found approximately in the same depth zone. Though there has been some

discussion as to whether the Central water can be regarded as a separate water mass, it is still found convenient to have a name for it. The Sub-tropical water occupies the upper 300 m of the water column in the southern channel while in the central Channel it is partly covered by Equatorial Surface water. Though these water masses mix and their characteristics are modified within the Mozambique Channel, a further division into new water mass categories seems artificial. As the seasonal salinity variation of the Equatorial Surface water is rather large, it is difficult to separate the Sub-tropical water and the Equatorial Surface water by a fixed salinity value.

Figure 25 shows tentative paths of propagation for the different water masses of the Mozambique Channel. There is some consistency between the routes of the water masses except for the North Indian Intermediate water.

Water masses along the Mozambique coast.

The water mass distribution along the Mozambique coast (Figure 26) is characterized by the presence of:

- a surface layer of water of Equatorial and Sub-tropical origins, partly mixed with coastal water, covering the upper 100 m.
- a sub-surface layer of Sub-tropical water, characterized by a salinity maximum at approximately 150-200 m resulting from the propagation of Sub-tropical water under Equatorial Surface water;
- a Central water layer, found at 400-500 m, corresponding to an oxygen maximum, the core of which is approximately coincident with the 11°C isotherm and the $35.0^{\circ}/\text{oo}$ isohaline;
- a layer of Antarctic Intermediate water the core of which rises from about 900 m in the south to 600 m in the north;

- a layer of North Indian Intermediate water, detectable in Figure 26 by a salinity maximum and an oxygen minimum present at 800-1000 m north of 18°S.

Figure 27 shows scattering t-S and t-O₂ diagrams for all the stations referred to in Table 1, except for the obviously wrong points which have been rejected. Low salinity values in the surface layer come from stations carried out over the shelf. In this chapter only the upper three depth zones of Figure 13 will be considered.

Surface waters

The characteristic parameters of the surface waters, per three month periods and per area (Figure 2), are presented in Table 9. Maximum surface temperatures were observed in February-April while minimum values were detected in August-September. The annual range of surface temperatures is 2-5°C, regardless of area. For each quarter of the year the temperature in area A is usually 2-5°C higher than in area E.

Maximum salinity values in areas A and B were observed in September-October, when the divergence of the South Equatorial current was in its northernmost position. Minimum values were detected in March-April when the water of Equatorial origin was exerting its maximum influence.

In area C there is an apparent seasonal trend in the salinity variations off the shelf (Table 9) following the average trend of the river runoff (Figure 10). As previously mentioned the main contributor of freshwater in area C is, by far, the Zambezi River which shows a non-seasonal trend (Figure 11). A hydrographic section repeated eight times during March 1980 (ANON 1981), revealed a salinity range off the shelf from 34.8‰ to 35.4‰ during twelve days. These facts suggest that short-term variability is probably more significant than the seasonal variations of the surface salinity in area C.

Maximum salinities were found in area D in July-August, while minimum values occurred in March, when the influence of modified Equatorial Surface water was greatest. Except for January-March, area E shows approximately the same salinity range throughout the year. Area D often contained pockets of low salinity (below $35.0^{\circ}/\text{oo}$) water (Figures 30c and 39), which were most likely due to southward transport of water from the Sofala Bank.

Immediately below the surface homogeneous layer a salinity minimum was often found (Figure 28a). Table 10 reveals that its presence can be detected all over the year, being less frequent in the third quarter and in area B.

Oxygen values at the surface varied roughly between 4.4 ml/l and 5.4 ml/l for the whole of the Mozambican waters, the highest values being found in the south (areas D and E) and the lowest ones in areas B and C (Table 9). The seasonal trend is not quite clear, which might be due to the high scattering of the oxygen observations (Figure 27).

A shallow oxygen maximum has been observed near the bottom of the surface homogeneous layer (Figure 28b). This very weak maximum (oxygen values at the maximum were never found to exceed the surface values by more than 0.3 ml/l) has never been observed in area E or during the third quarter (Table 10). Usually its presence was associated with a decrease in the surface values from one quarter to the next.

Sub-surface waters

At the sub-surface level two core layers can be identified (WYRTKI, 1971; LUTJEHARMS, 1972): a salinity maximum and an oxygen minimum usually found approximately in the same depth range (Figure 26). Generally speaking, one can say that both oxygen and salinity values showed an increase from north to south in each core layer (Tables 11 and 12). According to Figure 26, the oxygen minimum layer shows a reduction in thickness from north to south at the same time as its core tends to

be lifted, a feature that is not evident from Table 12, as only the extreme limits of the core layer are indicated there. From Figure 26 one can also see that in the north the cores of the salinity maximum and oxygen minimum are more or less coincident in depth, while in the south the core of the oxygen minimum layer tends to be situated above the salinity maximum. This feature agrees well with what is referred to by WYRTKI (1971).

No clear seasonal variations were observed in the salinity maximum, except in the northernmost area where, during the first quarter, salinities were higher than in area B. In the two southernmost areas the Sub-tropical water was often found to extend to the surface, e.g. Figure 29. This seems to be a characteristic feature of these areas.

The oxygen values in the sub-surface oxygen minimum showed no clear seasonal variations, which also agrees with WYRTKI (1971). However, interannual variations have been found, the oxygen values in 1977-1978 being approximately 0.5 ml/l lower than in 1978-1979 but these variations could also be explained in terms of systematic error in the sampling.

Figure 30 shows clearly that, in spite of the salinity maximum and the oxygen minimum being found in the same depth range, the highest salinities do not coincide with the lowest oxygen values. This was in fact a general tendency observed in almost all the sections: the two cores seem to "avoid each other". A similar situation can be observed in Figure 39 in which the two cores do not even show depth coincidence.

Central water

The near-linear relationship connecting points (8°C , $34.6^{\circ}/\text{oo}$) and (15°C , $35.6^{\circ}/\text{oo}$) in the t-S diagram was denominated Indian Ocean Central water by SVERDRUP et al. (1942). The t-S diagram of Mozambican waters, (Figure 27), closely follows that relationship, the scattering of the points falling fairly well within that expected by SVERDRUP et al. (1942).

Comparing the t - S and t - O_2 diagrams of Figure 27 one can see that the core of the intermediate oxygen maximum lies within the Central water, centered at 11°C , $35.0^\circ/\text{oo}$, corresponding to $\sigma_t = 26.80$, thus in agreement with DONGUY and PITON (1969), LUTJEHARMS (1972), ORREN (1966) and WYRTKI (1971).

Table 13 shows the characteristics of the intermediate oxygen maximum found in Mozambican waters at temperatures of 10 - 12°C . The values are in accordance with WYRTKI's (1971) atlas, which shows the oxygen maximum to be present in the Mozambique Channel at 400 - 500 m, the oxygen values decreasing northwards from more than 5.0 ml/l to 4.5 ml/l. No seasonal variations have been observed except in the southernmost area.

Discussion

The Mozambique Channel is a region of interaction of two surface water masses: the Equatorial Surface water and the Sub-tropical water. As previously mentioned it is difficult to ascertain characteristic values of these two water masses in the Mozambique Channel as they are highly modified in this region. On the other hand, there is a clear seasonal variation in the characteristics of Equatorial Surface water, as can be seen in DONGUY (1975). Figure 31 is believed to be a good example of the distribution of surface water masses in Mozambican waters. The influence of Equatorial water can be seen in this figure to extend to approximately 20°S (highest temperatures and lowest salinities). Off the shelf salinities below $35.0^\circ/\text{oo}$, supposedly characteristic of the more pure Equatorial surface water are, however, only found north of 15°S . The low salinity water detected in area C is clearly of coastal origin.

Sub-tropical water, as defined by ORREN (1963, 1966) and PEARCE (1977) - i.e. with salinities above $35.5^\circ/\text{oo}$ - is present in the extreme south of the Mozambican waters (Figure 31). However, one can regard its influence as extending northwards to 21°S , corresponding to the $35.3^\circ/\text{oo}$ isohaline (LUTJEHARMS, 1971).

The shallow salinity minimum and oxygen maximum observed near the bottom of the surface homogeneous layer (Figure 28) are most likely the result of seasonal variations in surface conditions. They show clearly in the data from a fixed station in Malgasy waters presented by DONGUY and PITON (1969). In that paper the salinity minimum is shown to form after the period of lowest surface salinities. It sinks below waters of higher salinity and lasts until the next period of reduced surface salinity.

The shallow oxygen maximum will probably result from the decrease in surface values associated with moderate wind conditions and the high surface temperatures, characteristic of the north-east monsoon season. The intensification of the vertical mixing processes during the period of the strongest south-east trade winds will probably cause the salinity minimum and oxygen maximum to be less frequent in July-September.

The origin of the sub-surface salinity maximum, as well as its main routes of propagation, has already been discussed. In this chapter the authors will just try to provide additional evidence for its Sub-tropical origin.

Some authors tend to associate the sub-surface salinity maximum with the sub-surface oxygen minimum to postulate a "south equatorial origin" (KHIMITSA, 1968; IVANENKOV and GUBIN, 1960; ISAENKO et al., 1980) or an "Arabian sea origin" (ROCHFORD, 1964; MAGNIER and PITON, 1973) of the salinity maximum. WYRTKI (1962, 1971) stresses, however, the purely biochemical origin of the oxygen minima found in the ocean, their positions being determined by circulation, and avoids any association between oxygen minima and salinity maxima. In the present authors' opinion this is the most fruitful approach, as it allows us to regard the two extremes as independent. From this point of view, the apparent southward propagation of the oxygen minimum (Figure 26) is quite expectable once the main currents in the western Mozambique Channel become southbound.

As mentioned before, the general trend is for a "mutual avoidance" of highest salinities and lowest oxygen values in the two core layers (Figure 30), and this trend is clear both in the south and in the north, suggesting that the salinity maximum proceeds from a region of high oxygen content. The only such region in the Indian Ocean is the southern sub-tropical gyre, and thus the sub-surface salinity maximum will be taken as the core of the Sub-tropical water, which propagates under the Equatorial Surface water. The apparent southward propagation of this core in the north (Figure 26) can be explained in terms of Sub-tropical water that enters the Mozambique Channel around the northern tip of Madagascar, as previously suggested by MAGNIER and PITON (1974). The greatest erosion of the core layer will then happen in the narrowest part of the channel, between 15°S and 17°S, as suggested by Figure 26 and referred to by HARRIS (1972).

An additional support for the Sub-tropical origin of the salinity maximum is the consistency between the routes of propagation of this core layer with those of the intermediate oxygen maximum - Central water - and the intermediate salinity minimum - Antarctic Intermediate water. Figures 26 and 32 clearly support this consistency, which has already been indicated in Figure 25.

CIRCULATION

Circulation pattern along the Mozambique coast

According to the strict $t-\sigma_t$ relationship shown by Figure 4 and Table 3, indications on the circulation pattern of the upper layers off Mozambique may be visualized by the temperature distribution at 150 m depth. Figures 33 and 34 demonstrate examples of this.

Along the Mozambican coast the circulation pattern seems to be characterized by the influence of three anti-cyclonic cells changing their position along the coast, and some smaller cyclonic eddies. Figure 35 shows the approximate position of

these features. For convenience, the cells have been numbered I, II and III while the eddies are called a, b, c, d and e. In this figure the circulation features are shown as fully developed. This was found convenient for elucidation purpose although it does not represent any observed situation.

In December 1978 (Figure 33a) the three anti-cyclonic cells were clearly identifiable. Cell I was limited to the north by the divergence of the South-Equatorial Current situated at 11° - 12° S. Eddy a was fully developed and separated Cells I and II. Eddy b is regarded as a shelf process and is most likely a result of the Zambezi outflow. Eddy e was situated rather near the coast while eddy c was reduced to a cyclonic curvature of the isolines. Eddy d was not seen due to poor data coverage in that area.

In December 1980 (Figure 33b) the anti-cyclonic cells seemed to have a more southerly position. Cell III could hardly be seen. The cells were not pronounced in February-March 1978 probably due to lack of more offshore data (Figure 33c). Eddy a was displaced closer to the coast in February-March both in 1978 and in 1980 than in December 1978. Eddy e was found more offshore in February-March 1980 than in December 1980. Eddies c and d was clearly detectable in February-March 1978. During the same period in 1980, however, the data coverage in the nearshore area was probably too poor to show these features.

In May-June 1979 (Figure 33d) only cell III could be clearly identified. All dynamic features had lower intensities than in December 1978. Eddy a was reduced to a cyclonic curvature of the isolines. Eddy d was clearly observed. A wide cyclonic area was present between 22° and 24° S with eddy e being still detectable. Apparently only one anti-cyclonic cell was influencing the northern and central parts of the western Mozambique Channel while cell III was still present in the south.

In August 1980 (Figure 34a) eddy a could not be observed at all. Indications of cells II and III were present. Eddy c seemed to

be rather developed while eddy e was displaced southward compared to December 1978 and May-June 1979.

In September 1978 (Figure 34b) eddy c was probably found close to the coast at about 21°S. An anti-cyclonic eddy was found stretching between 22° and 25°S. This eddy might have been remains of what have previously been referred to as cell II, or a northward transport and shedding of a part of cell III. During this cruise the observations north of 15°S had to be deleted due to obviously wrong values. However, an anti-cyclonic cell seemed to be extending from the north of the Channel to about 18°S. Indications of the presence of eddy e were observed in the extreme south-east of the investigated area.

The available data lend some support to a concept of seasonal variations in the most conspicuous circulation pattern, with a separation of the anti-cyclonic cells I and II during southern summer and a more or less continuous current in the northern and central part as typical for the southern winter.

The observed cyclonic eddies were deep, reaching down to more than 500 m. The characteristic horizontal extensions of the eddies were 150 km for eddies c and d while eddy a extended about half this distance. The eddies usually had their strongest baroclinic structure below 200 m. Figure 36 shows a hydrographic section across eddy a during a period when it was hardly observed by the temperature in 150 m (Figure 33d). Figure 37 shows a section across eddy c during the same cruise. The apparent intensification of the eddies during the southern summer, as observed in the temperatures at 150 m, seemed to be related to a lifting of the baroclinic structure during this period.

Eddy d was first reported by ORREN (1963) and eddy a was observed by HARRIS (1972). They both appear to be quasi-stationary. The hydrographic sections of ATLANTIS II in 1963 and 1965 along the 26°S parallel showed eddy d clearly (JORGE DA SILVA et al. 1981). Research carried out in the area of eddy d in January 1982 strongly indicated this to be topographically induced. It seems likely that this is also the case for eddy a.

The circulation patterns shown in Figures 33-35 clearly demonstrate the difficulties one has to face when trying to reveal seasonal variations in the Mozambique Current by means of geostrophic calculations. However, the main parts of the hydrographic sections along the Mozambican coast showed their strongest baroclinic structure during the southern summer. Figures 33-35 do not provide any support to the established idea of a continuous Mozambique Current except perhaps during the southern summer.

On several occasions an inshore northward flow was observed along parts of the coast. It is uncertain if this is a continuous coastal current or only the western margin of the cyclonic eddies. Figure 38, showing a section across eddy a, is a typical example of a northward transport of low-salinity water near the coast. The counter current observed at the coastal side of the Agulhas Current seems not to be a permanent feature, and highly influenced by the prevailing winds (CLOWES, 1950). Occasionally, it has been observed to flow at high speeds (STAVROPOULOS and DUNCAN, 1974). Along the coast of Mozambique it is most frequently observed during March-April, i.e. the time of maximum freshwater runoff.

In the area 20° - 22° S a narrow band of southward moving low-salinity water is sometimes seen (Figure 39). Figure 30c shows another example. This water is due to the Zambezi outflow and may cause low surface salinities far from the coast south to about 24° S.

General features in the Mozambique Channel

Figure 40 shows the dynamic topography of the sea surface relative to the 500 decibar level from the six cruises covering the whole Mozambique Channel (Table 2).

The circulation in the northern part of the Channel seems to be dominated by an anti-cyclonic movement. This has been observed by several authors (DONGUY and PITON 1969, DUNCAN 1970, HARRIS

1972, LUTJEHARMS 1976, PARFENOVICH 1980, PITON, POINTEAU and NGOUMBI 1981). DONGUY and PITON (1969), however, claim this movement to be present only during the time of the north-east monsoon season while during the south-west monsoon season the water of the upper layers seemed to come from more southern parts of the Mozambique Channel.

Another anti-cyclonic movement seems to be characteristic for the central Mozambique Channel, with its center approximately at 20°S . This feature, also seen in HARRIS (1972) and LUTJEHARMS (1976), seemed to have the highest dynamic intensity during October-November 1957 and November-December 1952 (Figure 40). In July-August 1960 this anti-cyclonic movement was apparently absent. However, this could be explained by the lack of data along the Mozambican coast. During certain periods these two anti-cyclonic movements seemed to be connected.

On the eastern side of the Mozambique Channel it seems as if there is a southward-moving current near the coast of Madagascar, which is most pronounced south of 20°S . As can be seen in Figure 23a and c, this current seems to transport low-salinity water at surface. Sometimes the typical wedge-shape salinity distribution of a freshwater induced coastal current can be observed (Figure 23c). This southward flow was deduced by LUTJEHARMS (1971) and apparently confirmed by LUTJEHARMS (1981).

The anti-cyclonic gyre at the southern mouth of the Mozambique Channel, as reported by several authors, e.g. HARRIS (1972) was not clearly seen except in October-November 1957 and in April-May 1964. This might be explained by the poor data coverage of that area. Figure 40 indicate that the anti-cyclonic eddy stretching between 22° and 25°S in Figure 34b is most likely a result of the shedding of a part of cell III.

A continuous Mozambique Current is not made evident by Figure 40. Neither is the classical concept of the Agulhas Current as an extension of the Mozambique Current.

By comparing Figures 18 and 40 it seems that an upper layer outflow from the Mozambique Channel only occurred in April-May 1964 and in July-August 1960. A clear blocking of the outflow was apparent during September 1962 and September-October 1964. The situation during November-December 1952 and October-November 1957 was unclear as the two figures partly show contradicting results.

CONCLUSION

Based on the previous presentation, Figure 41 gives tentative circulation patterns in the upper layers of the Mozambique Channel.

During the southern summer, there seems to exist an anti-cyclonic gyre in the northern part of the Channel (I), and another one in the central part, (II), separated by a cyclonic eddy a at 16° - 18° S (Figure 41b). During some parts of the year, most likely southern winter, these two anti-cyclones seem not to be separated. The northern anti-cyclone may then extend as an anti-cyclonic tongue into the central parts of the Channel (Figure 41a).

Between the anti-cyclones II and III, a cyclonic system, often consisting of the two eddies c and e, seems to be observed. Occasionally, the anti-cyclone III may extend a tongue towards north reaching 21° - 22° S or approximately the position of the 3000 m isobath (Figure 3). Another tongue, which is also regarded as part of the anti-cyclone III, is sometimes seen off the southern part of Mozambique (Figure 41a). Occasionally, this tongue seems to be able to separate from the anti-cyclone III giving rise to a stretched anti-cyclonic cell at 22° - 26° S west of 38° E (Figure 34b).

The cyclonic eddies a and d appear to be quasi-stationary and are most likely topographically induced. Eddy b is considered as a shelf process resulting from the outflow of the Zambezi River. Eddies c and e seem to form a moving cyclonic system.

The general circulation system of the Mozambique Channel is apparently highly conditioned by the topography. The pattern of Figure 4lb seems to offer the best fit to the water mass distribution below the surface layer and above the North Indian Intermediate water. Eddy a has been observed to be present also during the southern winter even if was hardly seen in the temperature distribution in 150 m. The pattern of Figure 4la may therefore only represent the modifications in the surface layer, especially during southern winter, due to the influence of the prevailing winds.

An inshore northward current seems to be present along most of the Mozambican coast, probably as a result of presence of the cyclonic eddies. It is not clear, however, if this coastal current is a continuous one.

The present results strongly indicate that in the upper 1000 m the role of the Mozambique Current as one of the tributaries to the Agulhas Current is of minor significance and question the concept of the Mozambique Current as a continuous one.

REFERENCES

- ANON. (1977). Atlas Okeanov - Tom 2 Atlanticeskij i Indijskij Okeany - Ministerstvo Oborony SSSR Voenno-Morskoj flot - Moskva 1977.
- ANON. (1981). Die ozeanologischen Bedingungen im Westteil des Mocambiquekanals im Februar/März 1980. (Abschlussbericht), 241 pp. Institut für Meereskunde der Akademie der Wissenschaften der DDR, Rostock-Warnemünde, 241 pp.
- ATAÍDE, C. (1981). A água na República Popular de Moçambique. Construir, 5: 4-11.
- BRINCA, L., REY, F., SILVA, C. and SETRE, R. (1981). A survey on the marine fish resources of Mozambique, Oct.-Nov. 1980. Reports on surveys with the R/V Dr. Fridtjof Nansen. Instituto de Desenvolvimento Pesqueiro, Maputo. Institute of Marine Research, Bergen. 58 pp.

- BURKOV, V.A. and KUKSA, V.I. (1977). Intermediate waters of the world ocean. Trudy VNIRO, 119: 39-45.
- CLOWES, A.J. (1950). An introduction to the hydrology of South African waters. Fisheries and Marine Biological Survey Division, Union of South Africa, Investigational Report No. 12: 42 pp.
- CLOWES, A.J. and DEACON, G.E.R. (1935). The deep-water circulation of the Indian Ocean. Nature, 136: 936-938.
- DARBYSHIRE, J. (1964). A hydrological investigation of the Agulhas Current area. Deep-Sea Research, 11: 781-815.
- DARBYSHIRE, M. (1966). The surface waters near the coasts of Southern Africa. Deep-Sea Research, 13: 57-81.
- DONGUY, J.R. (1975). Les eaux superficielles tropicales de la partie occidentale de l'Océan Indien en 1966-1967. Cahiers O.R.S.T.O.M., Série Océanographie, 13(1): 31-47.
- DONGUY, J.R. et PITON, B. (1969). Aperçu des conditions hydrologiques de la partie nord du canal du Mozambique. Cahiers O.R.S.T.O.M., Série Océanographie, 7(2): 3-26.
- DUNCAN, C.P. (1970). The Agulhas Current. Ph.D. dissertation, University of Hawaii, 76 pp.
- GRUNDLINGH, M.L. (1977). Drift observations from NIMBUS VI satellite-tracked buoys in the south-western Indian Ocean. Deep-Sea Research, 24: 903-913.
- HARRIS, T.F.W. (1972). Sources of the Agulhas Current in the spring of 1964. Deep-Sea Research, 19: 633-650.
- HARRIS, T.F.W., LEHECKIS, R. and van FOREEST, D. (1978). Satellite infra-red images in the Agulhas Current System. Deep-Sea Research, 25: 543-548.

- IVANENKOV, V.N. and GUBIN, F.A. (1960). Water masses and hydrochemistry of the western and southern part of the Indian Ocean. Transactions of the Marine Hydrophysical Institute, Academy of Science of the USSR, 22: 27-99.
- ISAENKO, L.A., LANIN, V.I., TYULEVA, L.S. and KORZUN, Y.V. (1980). Report on the work of the second Soviet-Mozambican Expedition on fisheries research (August 1978 to September 1979). AzcherNIRO, Kerch.
- JORGE DA SILVA, A., MUBANGO, A. and SÆTRE, R. (1981). Information on oceanographic cruises in the Mozambique Channel. Revista de Investigaçãõ Pesqueira, N^o 2, 89 pp. Instituto de Desenvolvimento Pesqueiro, Maputo.
- KHIMITSA, V.A. (1968). On the water masses and hydrochemistry of the Mozambique Channel. Okeanologicheskii isledorania 19: 180-188.
- KUKSA, V.I. (1972). Some peculiarities of the formation and distribution of intermediate layers in the Indian Ocean. Oceanology, 12(1): 21-30.
- LE PICHON, X. (1960). The deep water circulation in the south west Indian Ocean. Journal of Geophysical Research, 65: 4061-4074.
- LUTJEHARMS, J.R.E. (1971). A descriptive physical analysis of water movement in the south west Indian Ocean during the north east monsoon season. M.Sc. Thesis, Univ. Cape Town.
- LUTJEHARMS, J.R.E. (1972). A quantitative assessment of the year-to-year variability in water movement in the South-west Indian Ocean. Nature Physical Science, 239(91): 59-60.
- LUTJEHARMS, J.R.E. (1976). The Agulhas Current system during the northeast monsoon season. Journal of Physical Oceanography, 6: 665-670.
- LUTJEHARMS, J.R.E. (1977). The need for oceanological research in the South-west Indian Ocean. South African Journal of Science, 73: 40-43.

- LUTJEHARMS, J.R.E., BANG, N.D. and DUNCAN, C.P. (1981). Characteristics of the currents east and south of Madagascar. Deep-Sea Research, 28A(9): 879-899.
- MAGNIER, Y. et PITON, B. (1973). Les masses d'eau de l'Océan Indien à l'ouest et au nord de Madagascar au début de l'été austral (novembre-décembre). Cahiers O.R.S.T.O.M., Série Océanographie, 11(1): 97-113.
- MAGNIER, Y. et PITON, B. (1974). Les particularités de la couche 0-600 m dans l'ouest de l'Océan Indien sud-équatorial. Cahiers O.R.S.T.O.M., Série Océanographie, 12(3): 143-158.
- MENACHE, M. (1963). Première campagne océanographique du Commandant Robert Giraud dans le canal de Mozambique, 11 octobre au 28 novembre 1957. Cahiers Oceanographiques, 15: 224-235.
- MUROMTSEV, A.M. (1950). Experimental regionalization of the world ocean. Trudy GOIN, No. 10.
- MUROMTSEV, A.M. (1977). Vertical structure of waters in the world ocean below the surface layer. Trudy VNIRO, 119: 46-58.
- ORREN, M.J. (1963). Hydrological observations in the south west Indian Ocean. South African Division of Sea Fisheries, Investigational Report No. 45: 61 pp.
- ORREN, M.J. (1966). Hydrology of the south west Indian Ocean. South African Division of Sea Fisheries, Investigational Report No. 55: 35 pp.
- PARFENOVICH, S.S. (1980). Hydrological features of productivity in the southwest part of the Indian Ocean. Trudy VNIRO, 145: 6-18.
- PEARCE, A.F. (1977). Some features of the upper 500 m of the Agulhas Current. Journal of Marine Research, 35: 731-751.

- PITON, B., POINTEAU, J.-H. and NGOUMBI, J.-S. (1981). Atlas hydrologique du Canal de Mozambique (Océan Indien). Travaux et Documents de l'O.R.S.T.O.M., No. 132: 41 pp.
- RAMAGE, C.S. (1969). Indian Ocean Surface Meteorology. Oceanography and Marine Biology, an Annual Review, 7: 11-30.
- ROCHFORD, D.J. (1964). Salinity maxima in the upper 1000 meters of the north Indian Ocean. Australian Journal of Marine and Freshwater Research, 15(1): 1-24.
- SHCHERBININ, A.D. (1969). Water structure of the equatorial Indian Ocean. Oceanology, 9: 487-495.
- STAVROPOULOS, C.C. and DUNCAN, C.P. (1974). A satellite-tracked buoy in the Agulhas Current. Journal of Geophysical Research, 79: 2744-2746.
- SVERDRUP, H.U., JOHNSON, M.W., and FLEMING, R.H. (1942). The Oceans, their physics, chemistry and general biology". Prentice Hall, New York.
- SÊTRE, R. and PAULA E SILVA, R. (1979). The marine fish resources of Mozambique. Reports on surveys with the R/V "Dr. Fridtjof Nansen". Servico de Investigações Pesqueiras, Maputo. Institute of Marine Research, Bergen. 179 pp.
- TINLEY, K.L. (1971). Determinants of coastal conservation: dynamics and diversity of the environment as exemplified by the Mozambique coast. Proceedings of the Symposium on Nature Conservation as a Form of Land Use, SARCCUS, Pretoria: 125-153.
- WYRTKI, K. (1962). The oxygen minima in relation to ocean circulation. Deep-Sea Research, 9: 11-22.
- WYRTKI, K. (1971). Oceanographic atlas of the International Indian Ocean Expedition. National Science Foundation, Washington D.C. 531 pp.

WYRTKI, K. (1973). Physical oceanography of the Indian Ocean. In: Biology of the Indian Ocean, B. Zeitzshel (editor), Springer-Verlag, Berlin, Heidelberg, New York, pp. 18-36.

Table 1. Number of stations performed in Mozambican waters, per area, season and year, from August 1977 to November 1980 (stations specifically chosen for shelf studies are not included). HS - hydrography station, BT - bathythermograph station.

AREA	NAME OF VESSEL	YEAR	JAN.-MAR.		APR.-JUN.		JUL.-SEP.		OCT.-DEC.		
			HS	BT	HS	BT	HS	BT	HS	BT	
A	Dr. Fridtjof Nansen	1977					7	23	7	18	
	Dr. Fridtjof Nansen	1978	7	24	7	25					
	Myslitel	1978					11	20			
	Nikolay Reshetnyak	1978							10	16	
	Ernst Haeckel	1979	9	-							
	Nikolay Reshetnyak	1979			10	15					
	Alexander von Humboldt	1980	36	-							
	Ernst Haeckel	1980					7	7			
	Dr. Fridtjof Nansen	1977					7	19	7	13	
	B	Dr. Fridtjof Nansen	1978	7	17	7	18				
Myslitel		1978					5	15			
Nikolay Reshetnyak		1978							5	8	
Ernst Haeckel		1979	6	-							
Nikolay Reshetnyak		1979			5	12					
Alexander von Humboldt		1980	28	-							
Ernst Haeckel		1980					44	46			
Dr. Fridtjof Nansen		1977					7	25	34	19	
C		Dr. Fridtjof Nansen	1978	30	29	31	55				
		Myslitel	1978					14	34		
	Nikolay Reshetnyak	1978							9	16	
	Ernst Haeckel	1979	7	-							
	Nikolay Reshetnyak	1979			13	20					
	Alexander von Humboldt	1980	87	-							
	Ernst Haeckel	1980					25	25			
	Dr. Fridtjof Nansen	1977					14	26	14	15	
	D	Dr. Fridtjof Nansen	1978	14	16	14	42				
		Myslitel	1978					14	25		
Nikolay Reshetnyak		1978							11	22	
Ernst Haeckel		1979	7	-							
Nikolay Reshetnyak		1979			14	19					
Alexander von Humboldt		1980	27	-							
Ernst Haeckel		1980					18	42			
Dr. Fridtjof Nansen		1977					6	23			
E		Dr. Fridtjof Nansen	1978	6	35	7	48				
		Myslitel	1978					7	11		
	Nikolay Reshetnyak	1978							7	10	
	Ernst Haeckel	1979	10	-							
	Nikolay Reshetnyak	1979			7	8					
	Alexander von Humboldt	1980	15	-							
	Ernst Haeckel	1980					23	32			
	Dr. Fridtjof Nansen	1980							28	-	
	Total		296	121	115	262	209	371	129	137	

Table 2. Previous cruises from which data have been used.
 CNEXO - Centre National pour l'Exploitation des
 Oceans, Brest - France.
 NODC - National Oceanographic Data Center,
 Washington, D.C. - USA.

NAME OF VESSEL	TIME	DATA SUPPLY
Alidade	Nov.-Dec. 1952	CNEXO
Commandant Robert Giraud	Oct.-Nov. 1957	MENACHE (1963)
" " "	Jul.-Aug. 1960	NODC
" " "	Sep.-Oct. 1962	"
Atlantis II	Oct.-Nov. 1963	"
" "	May -Jun. 1965	"
Almirante Lacerda	Apr.-May 1964	ANON (1965)
" "	Sep.-Oct. 1964	ANON (1967)
Ariel	Jul.-Aug. 1968	NODC

Table 3. Coefficients for the regression $\sigma_t = A + B \cdot t$. r = correlation coefficient
 n = number of pair of observations

	$t > 16^{\circ} C$				$t > 16^{\circ} C$ and $S > 35^{\circ}/\text{oo}$				$t \leq 16^{\circ}$			
	A	B	r	n	A	B	r	n	A	B	r	n
JAN.-MAR.	31.388	-0.323	0.980	479	30.835	-0.296	0.998	329	28.465	-0.149	0.963	176
APR.-JUN.	32.075	-0.363	0.661	520	30.751	-0.291	0.998	272	28.161	-0.127	0.965	196
JUL.-SEP.	30.846	-0.295	0.995	360	30.785	-0.292	0.995	335	28.136	-0.126	0.989	176
OCT.-NOV.	32.833	-0.390	0.427	466	30.837	-0.294	0.997	408	28.363	-0.142	0.969	119

Table 4. Factors for converting wind force ashore to wind force at sea, per prevailing wind direction, based on data from four selected coastal meteorological stations.

WIND DIRECTION	PEMBA	QUELIMANE	VILANCULOS	MAPUTO
NW	1			1.5-2
N				
NE		1	2	
E				
SE	1	1.5	1.5-3	2-4
S				

Table 5. Comparison of authors' average yearly runoff values of main rivers with similar data from ATAÍDE (1981).

RIVERS	PRESENT RUNOFF VALUES (km ³)	RUNOFF VALUES OF ATAÍDE (1981) (km ³)
ZAMBEZI	93.8	106.6
ROVUMA	-	12.6
LÚRIO	7.2	7.9
LICUNGO	6.6	7.0
PUNGOÉ	2.9	6.6
BUZI	5.9	6.6
SAVE	5.3	6.1
LIMPOPO	6.4	5.5
INCOMATI	2.4	3.9
MAPUTO	2.9	-
TOTAL (MAIN RIVERS)	133.4	162.8

Table 6. Seasonal characteristics of Mozambican rivers.

RIVER	FLOOD SEASON	PERCENTAGE OF TOTAL RUNOFF	FLOOD PEAK	PERCENTAGE OF TOTAL RUNOFF
Lúrio				
Melúli				
Ligonha				
Molocué	January-April	67-82	February-March	37-52
Melela				
Nipiode				
Licungo				
Incomati				
Umbeluzi	December-March	60-64	February	17
Maputo				
Zambezi (1960-1974)	January-April	56	February-March	32
Pungoé	December-April	74-84	February-March	42
Buzi				
Save	December-April	99	February-March	52
Limpopo	January-April	81	February-March	53

Table 7. Average, highest and lowest annual runoff values from four of the most important rivers (all available observational years up to 1980 have been considered).

RIVER	ANNUAL RUNOFF (Km ³)		
	AVERAGE	HIGHEST	LOWEST
Zambezi	77 (1960-80)	169 (1977-78)	40 (1972-73)
Buzi	7 (1956-77)	14 (1962-63)	1.5 (1967-68)
Save	7 (1960-80)	24 (1977-78)	0.4 (1967-68) (1972-73)
Limpopo	6 (1970-80)	14 (1977-78,	0.1 (1972-73)

Table 8. Various terminology of the water masses of the Mozambique Channel and South-western Indian Ocean.

		WATER MASS TERMINOLOGY	REFERENCES
Surface water		SOUTH EQUATORIAL/TROPICAL	(5, 6, 7, 10)
		TROPICAL/SUB-TROPICAL	(9, 14, 15, 18)
		AGULHAS/BOUNDARY	(3)
Sub-surface water		SOUTH EQUATORIAL SUB-SURFACE	(6, 7)
		SUB-TROPICAL SURFACE	(3, 14, 15, 20)
		SOUTH SUB-TROPICAL SURFACE	(13)
		NORTH EQUATORIAL/TRANSITION/TROPICAL	(10, 16)
		INTERMEDIATE SUB-SURFACE	(1)
		EQUATORIAL SUB-SURFACE/MOZAMBIKAN TROPICAL/SUB-TROPICAL	(5)
Central water		CENTRAL	(2, 3, 4, 9, 10, 14, 16, 19)
		SUB-TROPICAL SUB-SURFACE	(6, 7, 12)
		MAIN PYCNOCLINE	(1)
		EQUATORIAL	(9, 19)
Intermediate water	Low salinity	ANTARCTIC INTERMEDIATE	(1, 2, 4, 8, 10, 11, 14, 16, 19)
		SUB-ANTARCTIC INTERMEDIATE	(6, 7)
		SOUTH INDIAN INTERMEDIATE	(13)
	High salinity	RED SEA	(1, 4, 16, 17, 19, 20)
		ARABIAN SEA (INTERMEDIATE)	(10, 11, 13)
		NORTH INDIAN DEEP	(6, 7, 9, 14)
		NORTH INDIAN INTERMEDIATE	(21)

1. BURKOV and KUKSA (1977).
2. J. DARBYSHIRE (1964).
3. M. DARBYSHIRE (1966).
4. DONGUY and PITON (1969).
5. ISAENKO *et al.* (1980).
6. IVANENKOV and GUBIN (1960).
7. KHIMITSA (1968).
8. KUKSA (1972).
9. LUTJEHARMS (1971).
10. MAGNIER and PITON (1973).
11. MAGNIER and PITON (1974).
12. MUROMTSEV (1950).
13. MUROMTSEV (1977).
14. ORREN (1963).
15. PEARCE (1977).
16. PITON, POINTEAU and NGOUMBI (1981).
17. ROCHFORD (1964).
18. SHANNON (1967).
19. SVERDRUP *et al.* (1942).
20. WYRTKI (1971).
21. WYRTKI (1973).

Table 9. Distribution of surface characteristics per oceanic area and per quarter of the year for the period September 1977 - November 1980.

FEATURE	PERIOD	AREA				
		A	B	C	D	E
SURFACE TEMPERATURE (t°C)	JAN-FEB-MAR	28-31	26-30	27-30	26-30	26-29
	APR-MAY-JUN	27-30	27-29	26-28	25-27	24-25
	JUL-AUG-SEP	26-27	24-26	24-25	21-25	22-25
	OCT-NOV-DEC	27-29	26-28	27-28	26-28	25-27
SURFACE SALINITY (S ^o /oo)	JAN-FEB-MAR	34.3-35.2	34.5-35.0	34.4-35.3	34.4-35.2	34.4-35.2
	APR-MAY-JUN	34.7-35.1	34.5-35.1	34.0-35.3	34.5-35.5	35.0-35.5
	JUL-AUG-SEP	35.0-35.3	34.5-35.2	34.0-35.2	34.6-35.5	35.2-35.5
	OCT-NOV-DEC	34.8-35.2	34.5-35.2	35.0-35.4	35.2-35.4	35.3-35.5
SURFACE OXYGEN (O ₂ ml/l)	JAN-FEB-MAR	4.4-4.8	4.4-5.0	4.4-4.7	4.5-5.4	4.5-5.0
	APR-MAY-JUN	4.5-5.2	4.4-4.9	4.5-4.9	4.5-5.0	4.5-4.9
	JUL-AUG-SEP	4.5-5.1	4.7-5.1	4.6-5.1	4.6-5.0	4.8-5.3
	OCT-NOV-DEC	4.4-4.8	4.6-4.9	4.5-4.9	4.5-5.1	4.6-5.2
DEPTH OF HOMOGENEOUS LAYER (m)	JAN-FEB-MAR	20-80	10-70	30-40	20-60	30-80
	APR-MAY-JUN	20-120	10-80	30-90	30-90	50-100
	JUL-AUG-SEP	60-120	30-100	40-120	30-180	30-120
	OCT-NOV-DEC	30-100	20-80	30-80	20-80	20-80

Table 10. Recorded presence of the shallow salinity minimum and shallow oxygen maximum per quarter of the year and oceanic area. (When information was non-existent the place was left blank).

AREA	A				B				C				D				E			
	I	II	III	IV	I	II	III	IV	I	II	III	IV	I	II	III	IV	I	II	III	IV
SHALLOW SALINITY MINIMUM: + Present - Not Present																				
1977			-	-			-	+			-	-			-	+			-	
1978	+	-	-	-	-	-	-	-	+	-	-	+	+	-	-	+	-	+	-	+
1979	+	-			-	-			-	-			-	+			-	+		
1980	-				-	-			+	-			+	-			+		-	
SHALLOW OXYGEN MAXIMUM: + Present - Not Present																				
1977			-	-			-	+			-	+			-	+			-	
1978	+	+	-	-	+	-	-	-	+	+	-	+	-	-	-	+	-	-	-	-
1979	+	-			+	-			+	-			-	-			-	-		
1980	+				+	-			+	-			+	-			-		-	

Table 11. Distribution of salinity, temperature and depth at the core layer of the subsurface salinity maximum, per oceanic area.

AREA	SALINITY AT CORE LAYER		LIMITS	TEMPERATURE AT CORE LAYER	DEPTH (m) OF CORE LAYER
	JAN-MAR	JUL-SEP			
A	35.30-35.50	35.25-35.35	Upper	21-22	100-150
			Lower	13-14	300-400
B	35.25-35.45		Upper	20-21	100-150
			Lower	14	300-400
C	35.35-35.50		Upper	20-22	50-200
			Lower	13-15	300-350
D	35.35-35.55		Upper	19-22	50-100
			Lower	13-14	250-400
E	35.40-35.60		Upper	20-22	50-100
			Lower	14-16	300-400

Table 12. Distribution of oxygen, temperature and depth at the core layer of the subsurface oxygen minimum, per oceanic area.

AREA	OXYGEN (ml/l) AT CORE LAYER	LIMITS	TEMPERATURE AT CORE LAYER	DEPTH (m) OF CORE LAYER
A	2.5-3.7	UPPER	20-21	120-170
		LOWER	14-15	260-330
B	2.7-3.7	UPPER	20-22	50-200
		LOWER	14-15	300
C	2.7-3.7	UPPER	20-21	75-150
		LOWER	15-16	200-300
D	3.0-4.6	UPPER	20-22	50-150
		LOWER	14-16	250-350
E	3.3-4.5	UPPER	20-21	70-100
		LOWER	15-16	200-320

Table 13. Distribution of oxygen and depth at the core layer of the intermediate oxygen maximum, per oceanic area.

AREA	A	B	C	D	E
OXYGEN (ml/l) AT CORE LAYER	4.3-4.9	4.0-4.8	4.0-4.9	4.3-5.4	JAN-MAR JUL-SEP
					4.4-4.6 4.5-5.4
DEPTH RANGE (m) OF CORE LAYER	400-500	400-500	300-500	400-500	300-500

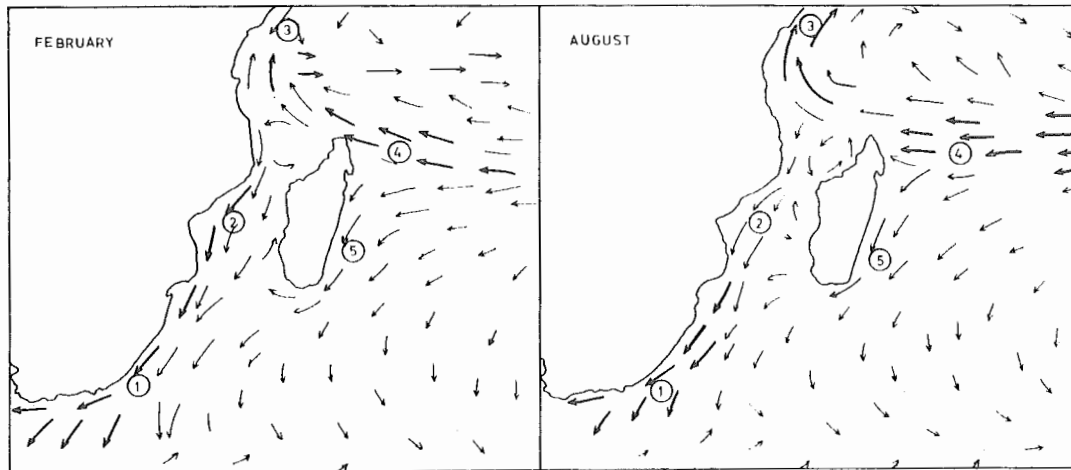


Fig. 1. Surface currents of the south-west Indian Ocean for February and August (ANON, 1977).

- | | |
|-----------------------------|------------------------------|
| 1) Agulhas Current. | 2) Mozambique Current. |
| 3) Somali Current. | 4) South Equatorial Current. |
| 5) East Madagascar Current. | |

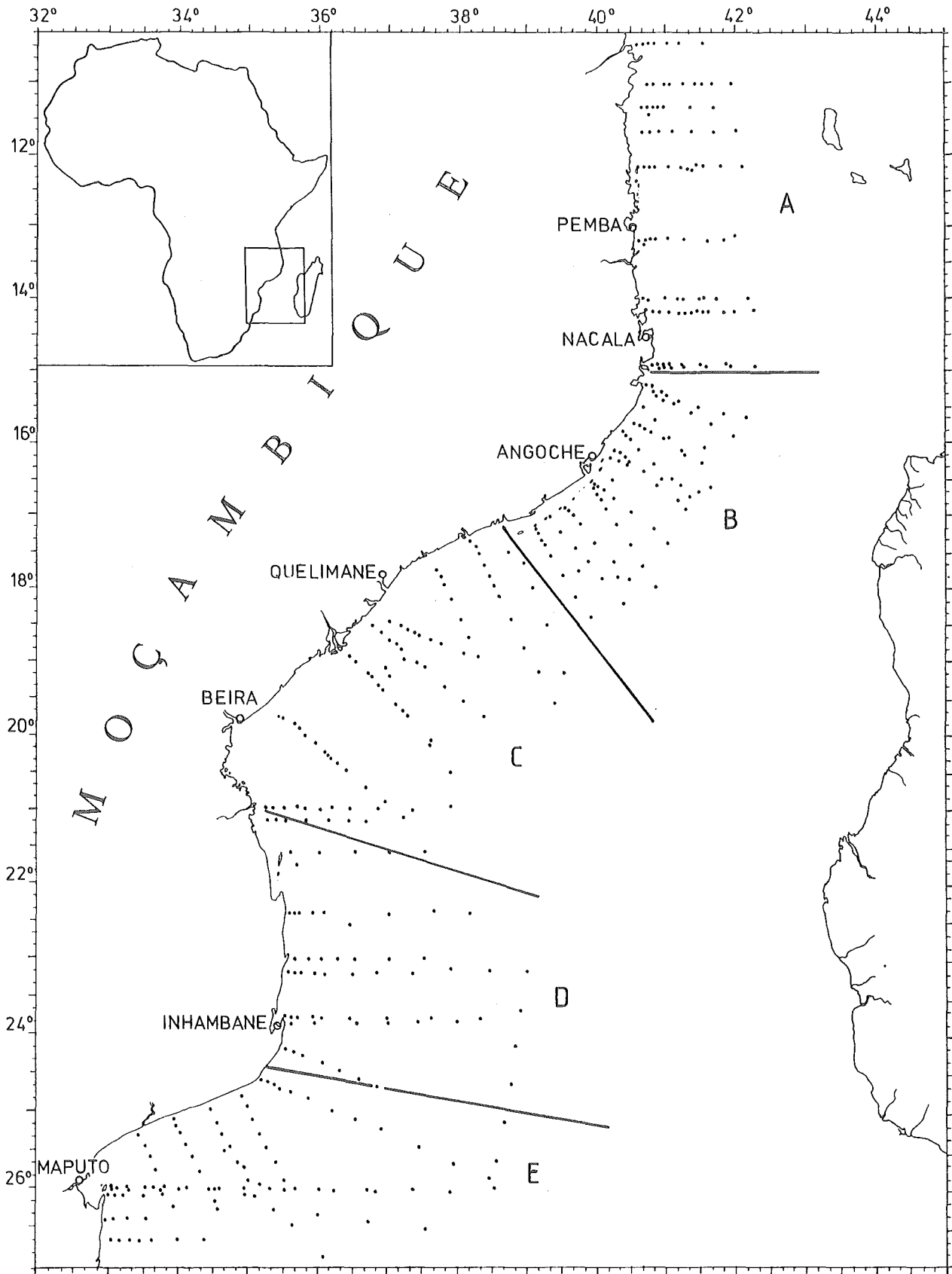


Fig. 2. Distribution of hydrographic stations from 1977-1980, divided into . sub-areas. Repeated sections are indicated only once.

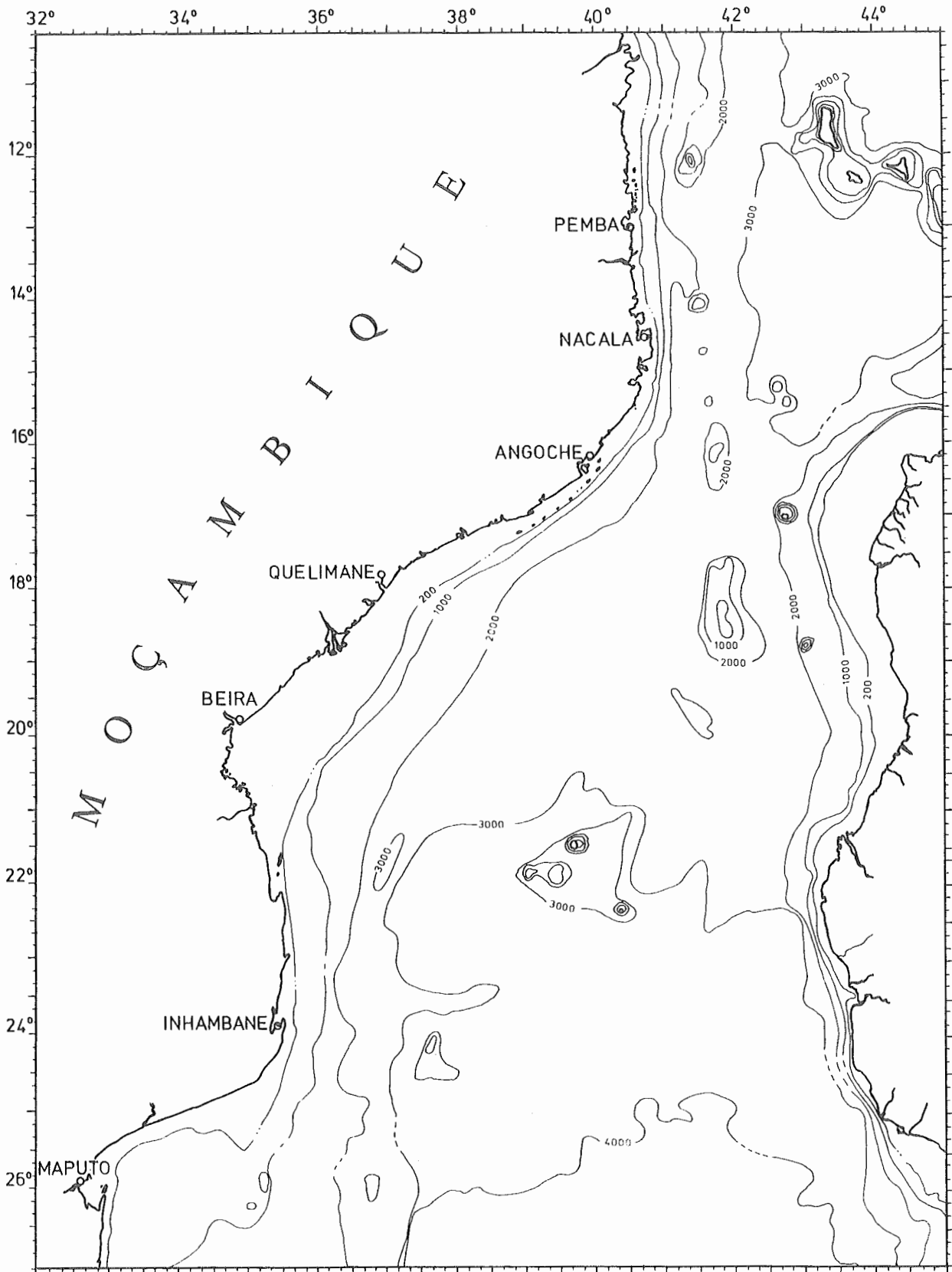


Fig. 3. Bathymetric map of the Mozambique Channel. Depth in meters.

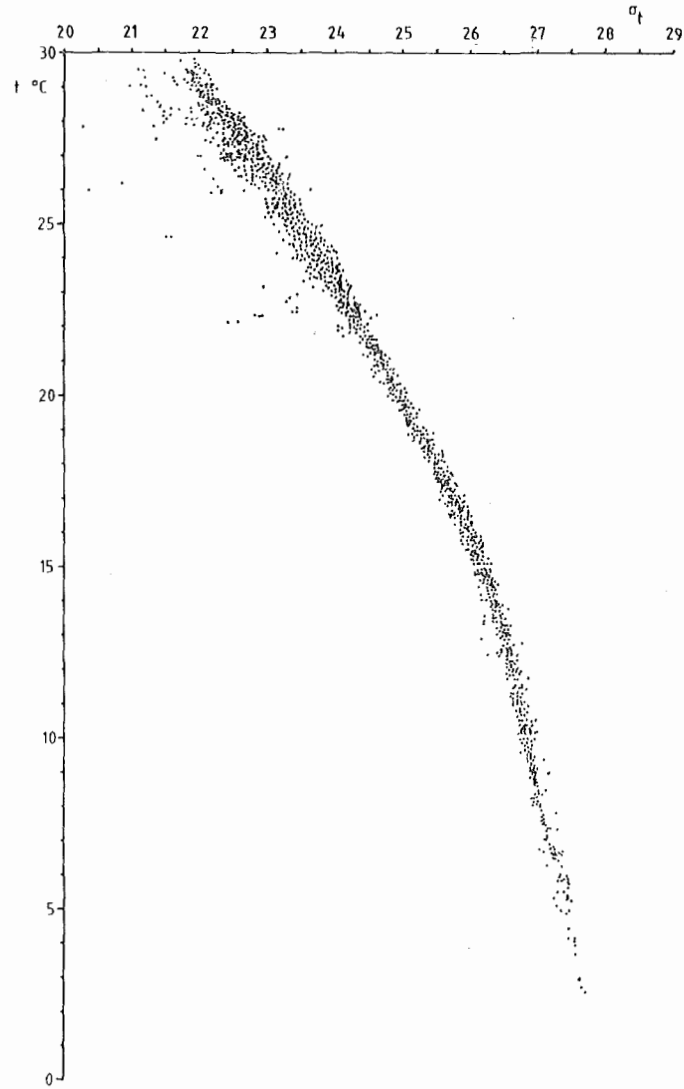


Fig. 4. σ_t - t scattering diagram for the hydrographic data 1977-1980.

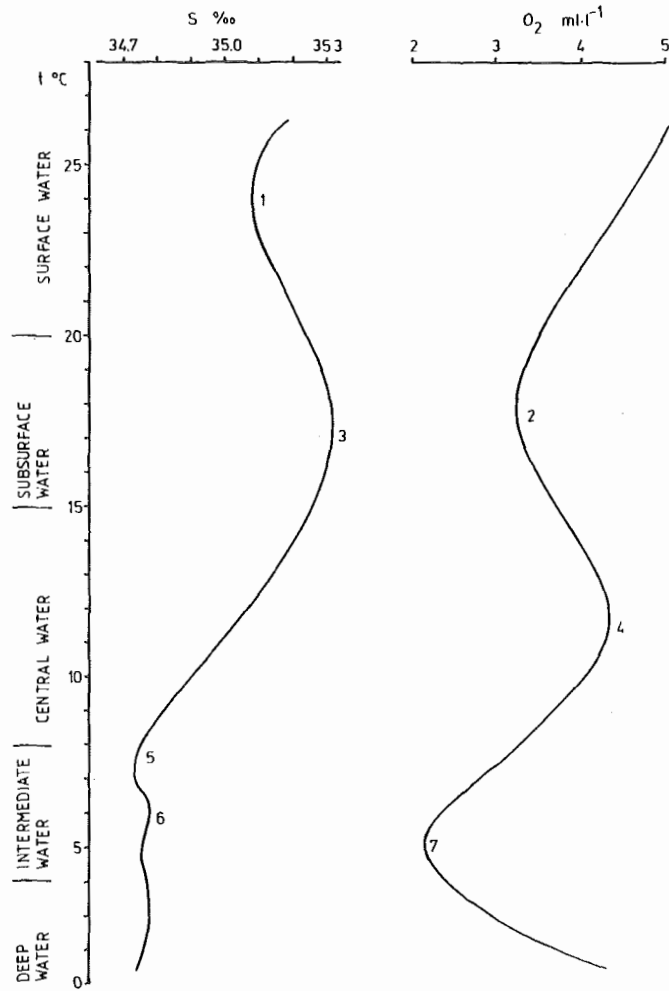


Fig. 5. Simplified t-S and t-O₂ diagram for the Central Mozambique Channel (B = structure).

1. The shallow salinity minimum.
2. Subsurface oxygen minimum.
3. Subsurface salinity maximum.
4. Intermediate oxygen maximum.
5. Intermediate salinity minimum.
6. Intermediate salinity maximum.
7. Deep oxygen minimum.

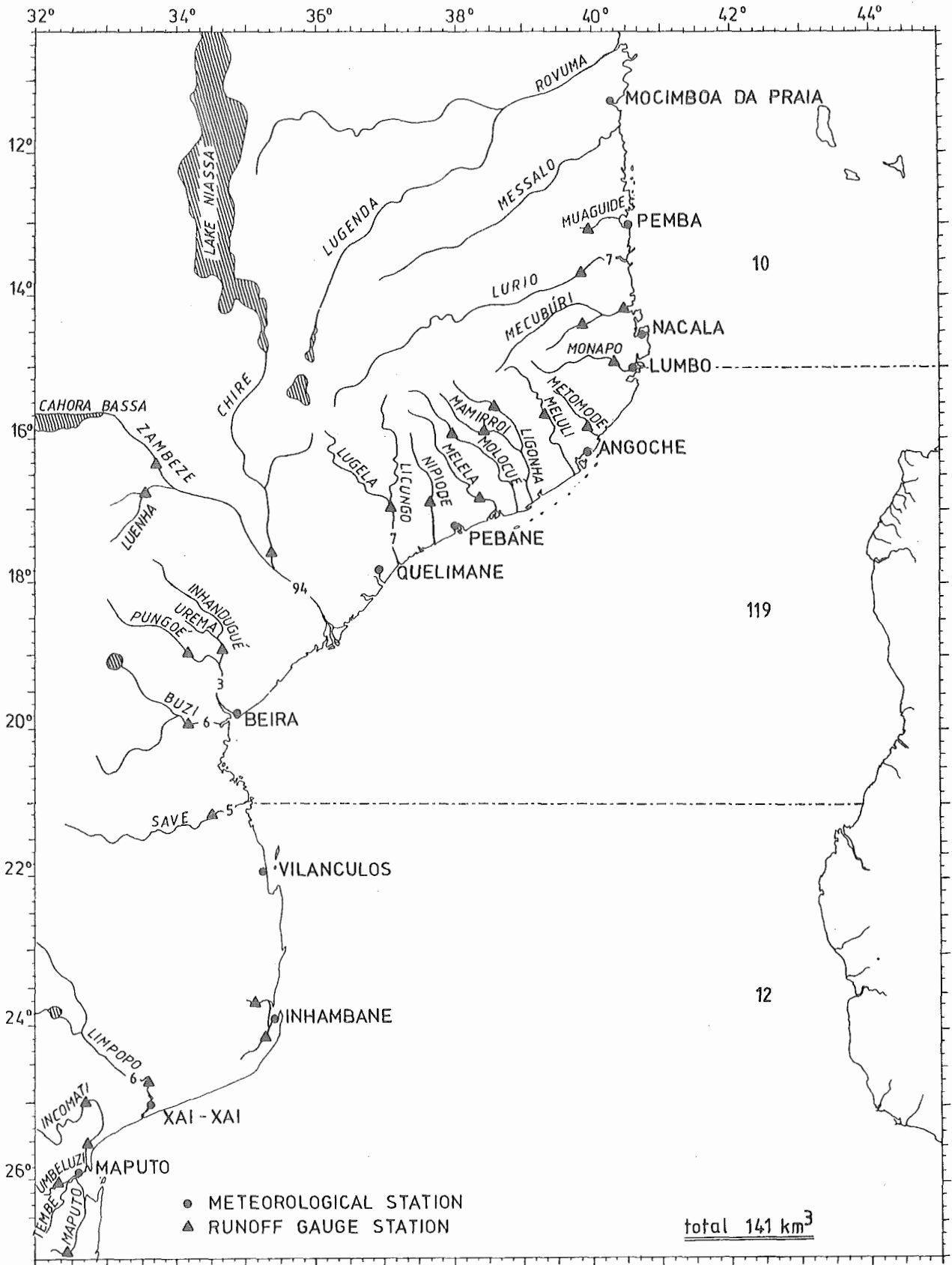


Fig. 6. Mean annual freshwater runoff (km³) and the location of meteorological and runoff gauge stations.

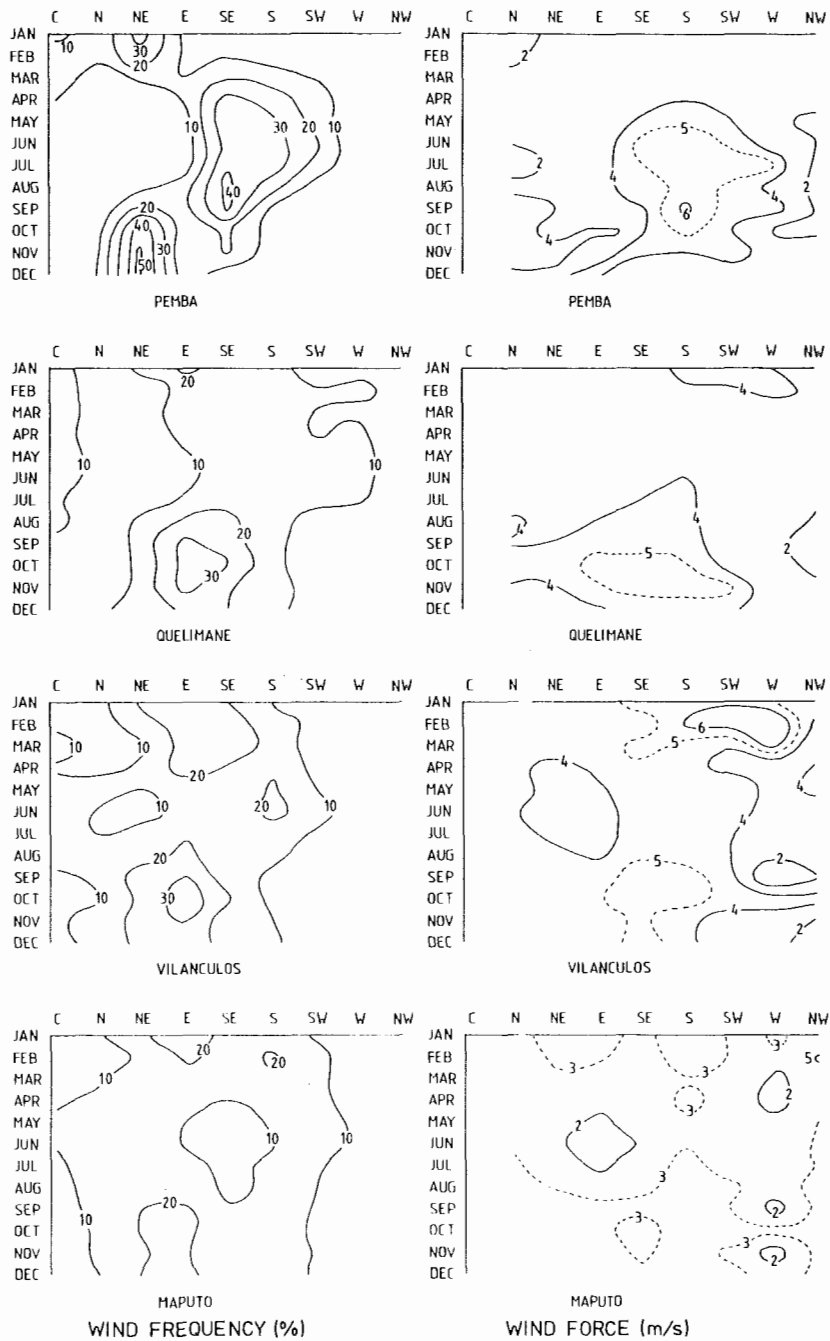


Fig. 7. Mean monthly distribution of wind direction (%) and force (m/s) at four selected coastal stations for the mean year 1968-1977.

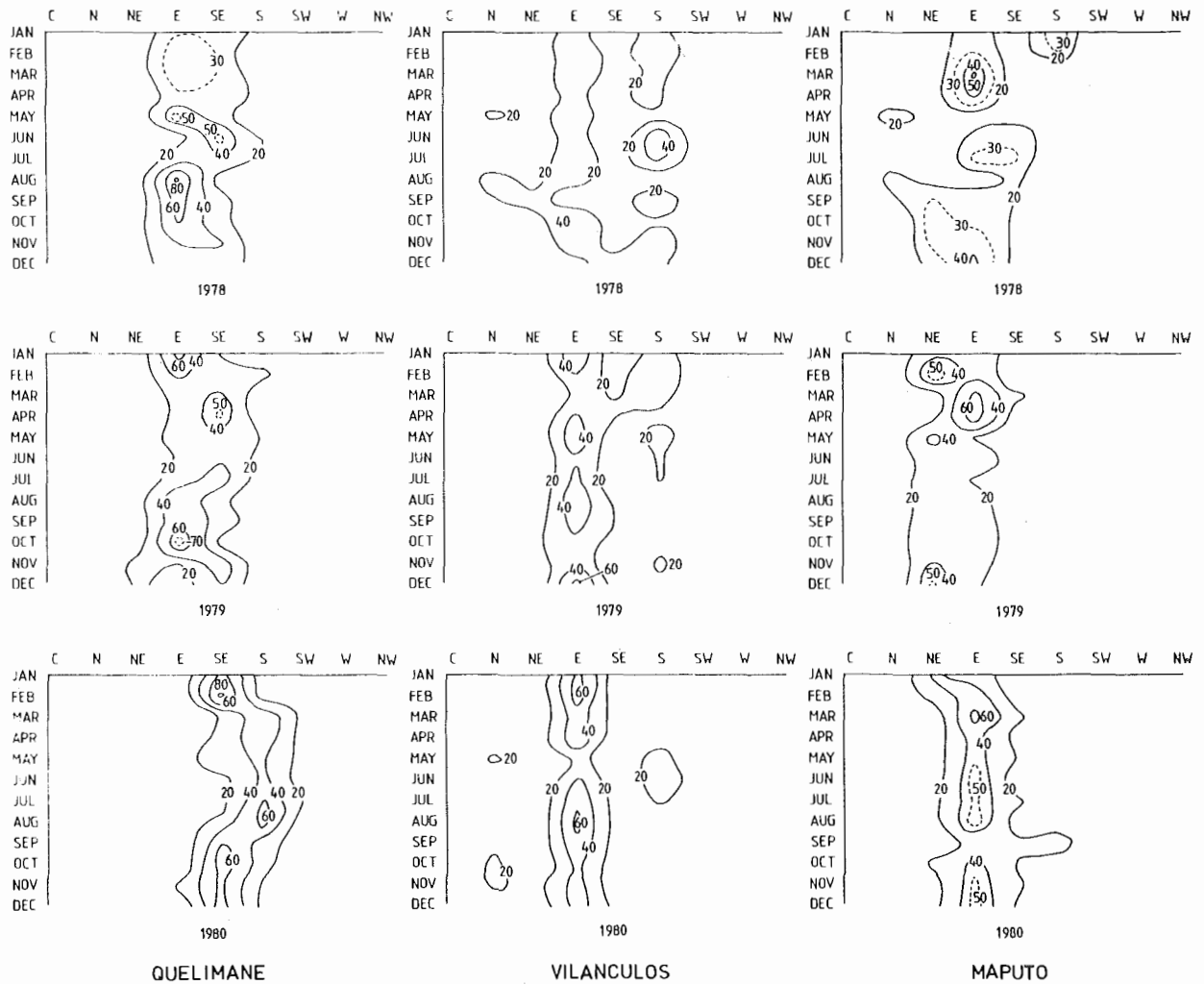


Fig. 8. Monthly distribution of wind direction (%) in central and southern Mozambique at 1500 hours for 1978, 1979 and 1980.

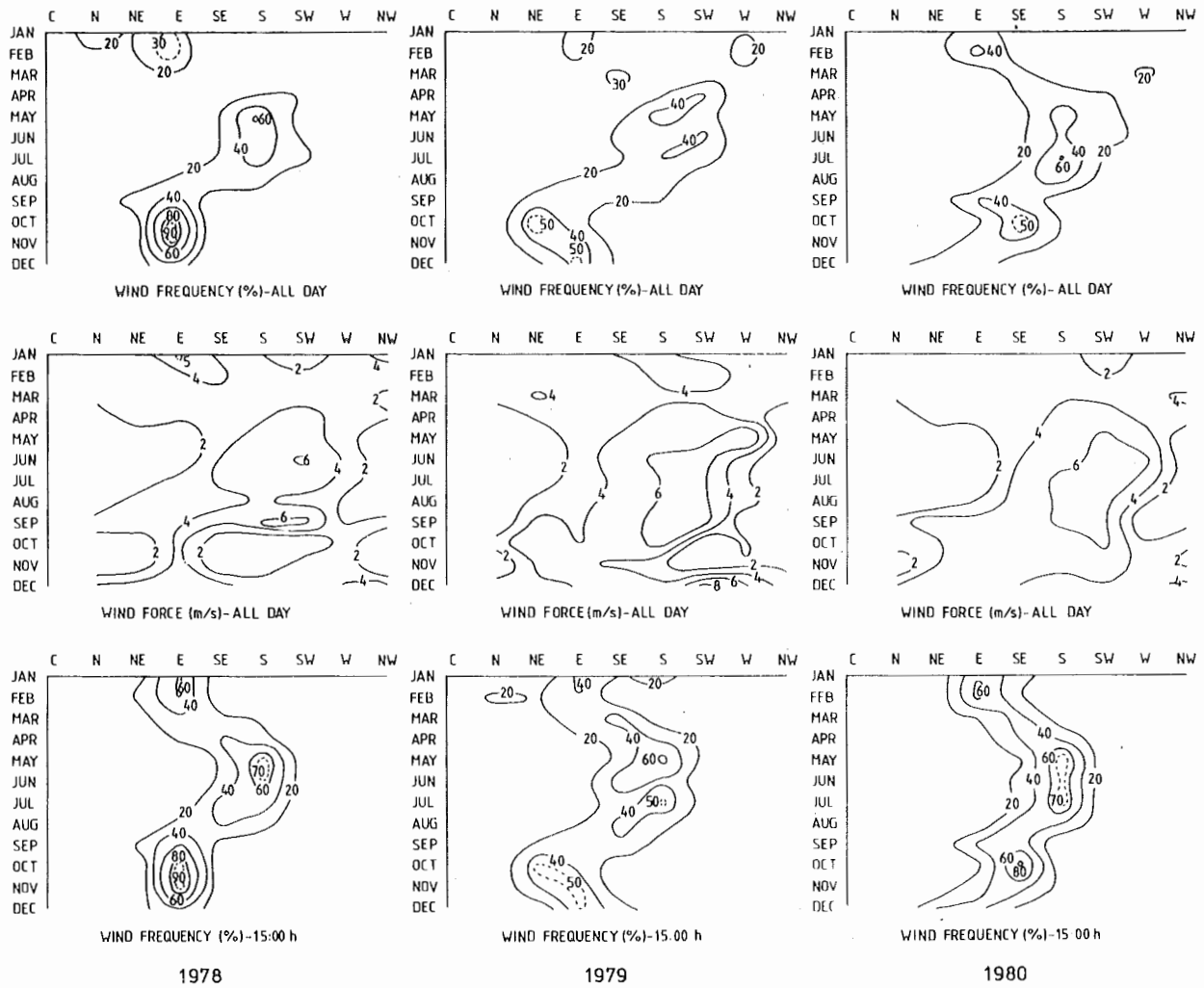


Fig. 9. Monthly distribution of wind direction (%) and force (m/s) in northern Mozambique (PEMPA) for 1978, 1979 and 1980. Comparison of all-day wind frequencies with wind frequencies at 1500 hours.

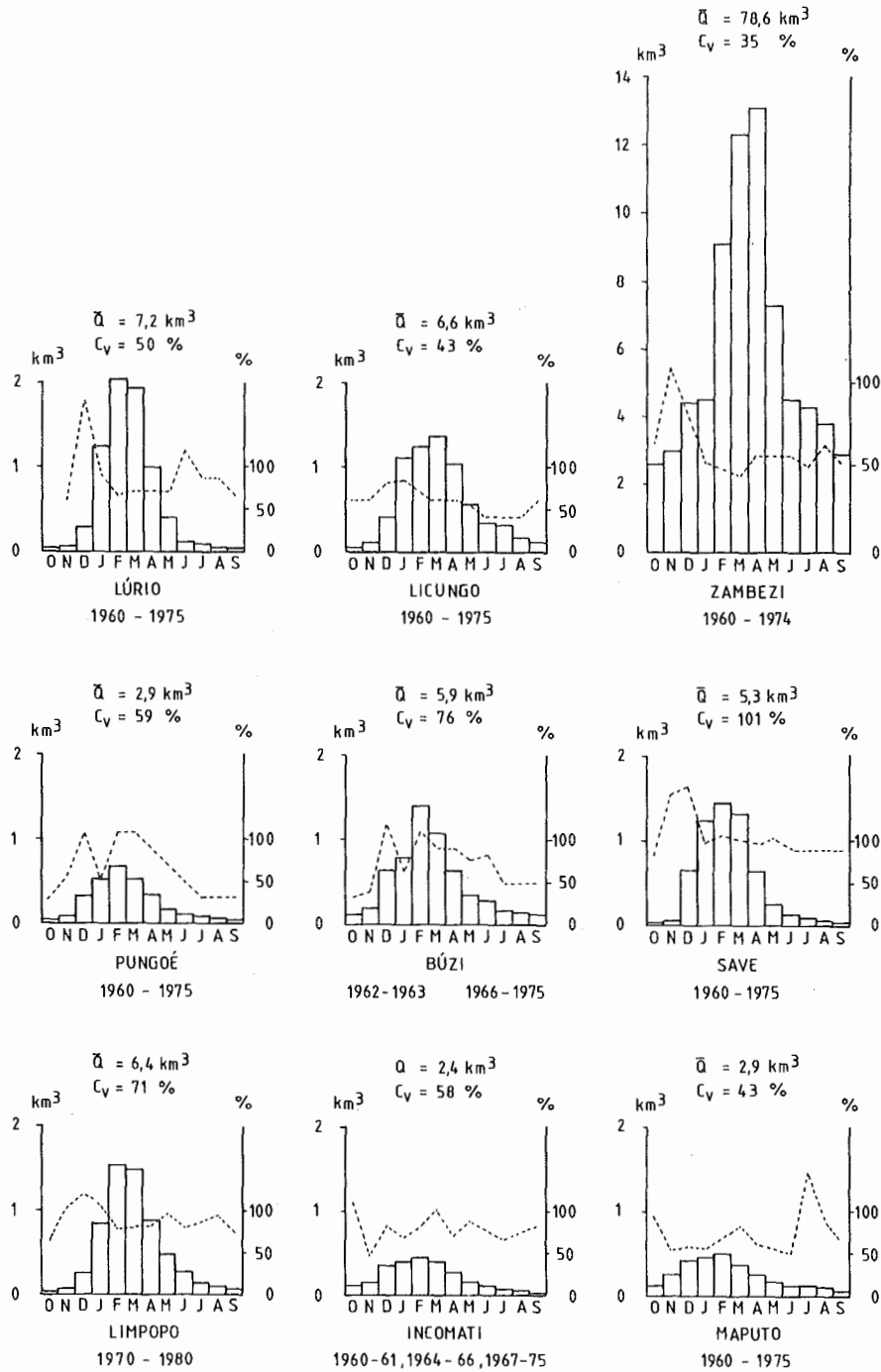


Fig. 10. Monthly means of the freshwater runoff for some main rivers, \bar{Q} . Dotted line is the variability coefficient, C_v , in percent.

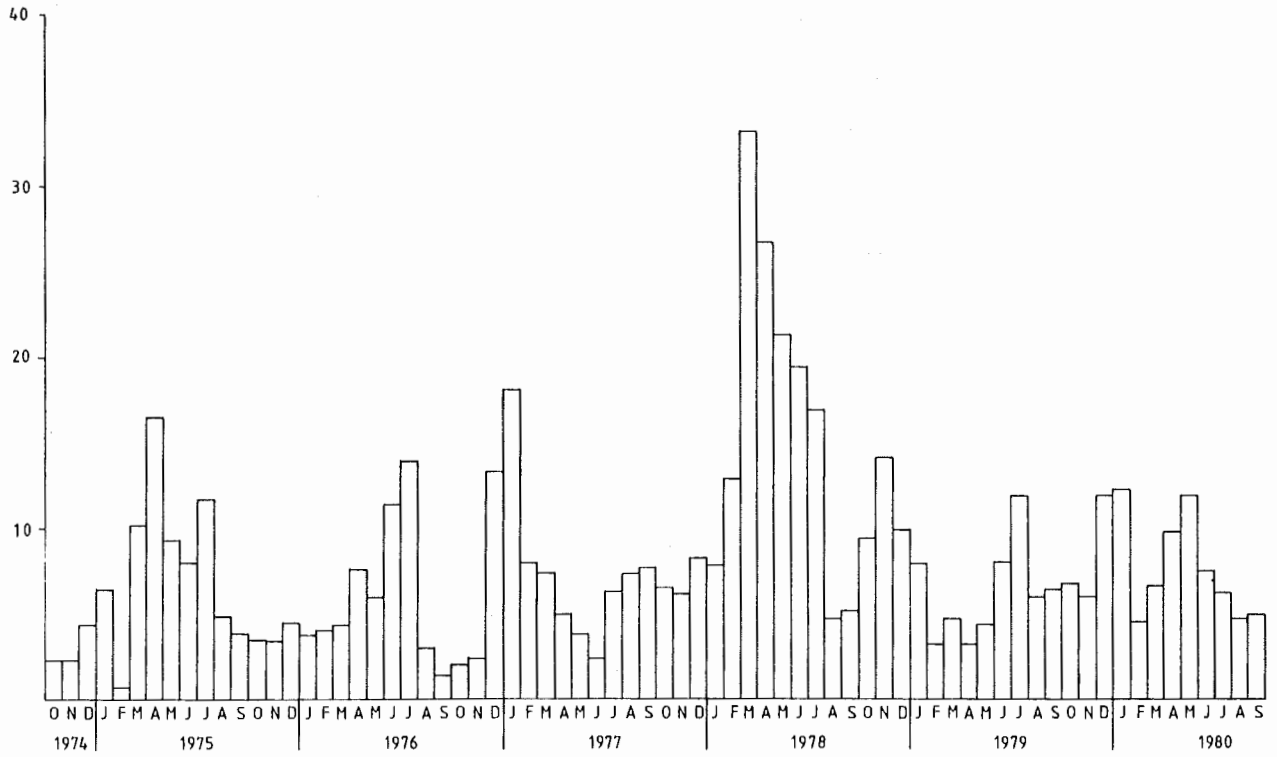


Fig. 11. Monthly runoff values from Zambezi River at Tete (km³), 1974-1980.

AUTHORS	SVERDRUP et al (1942)	IVANENKOV and GUBIN (1960)	SHCHERBININ (1969)	KUKBA (1972)	BURKOV and KUKBA (1977)
20°N	INDIAN OCEAN EQUATORIAL WATER	NORTH EQUATORIAL ZONE		PERSIAN/ARABIAN STRUCTURE	ARABIAN STRUCTURE
10°N				RED SEA/ARABIAN STRUCTURE	
0°			ARABIAN SEA STRUCTURE		EQUATORIAL STRUCTURE
10°S	INDIAN OCEAN CENTRAL WATER	SOUTH EQUATORIAL ZONE	EQUATORIAL STRUCTURE	EQUATORIAL STRUCTURE	SOUTH SUBTROPICAL STRUCTURE
20°S			SOUTH TROPICAL STRUCTURE	WEST MADA- GASCAR VARIETY STRUCTURE	
30°S		TROPICAL ZONE			
40°S		SUBTROPICAL ZONE		SOUTH SUBTROPICAL STRUCTURE	SUBANTARCTIC STRUCTURE

Fig. 12. The varied terminology of the water structure of the Indian Ocean.

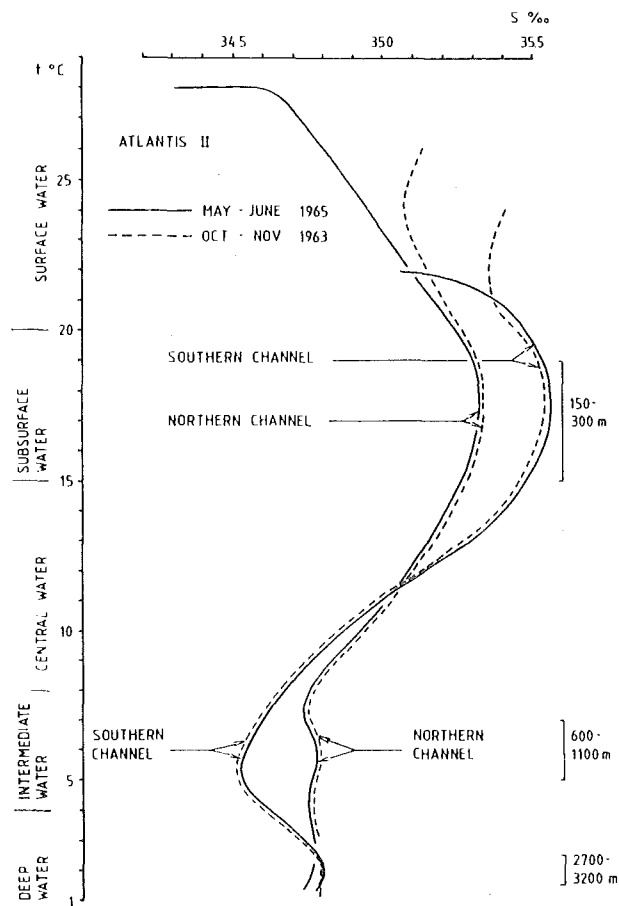


Fig. 13. Smoothed t-S curves from the cruises of ATLANTIS II in May-June 1965 and October-November 1963.

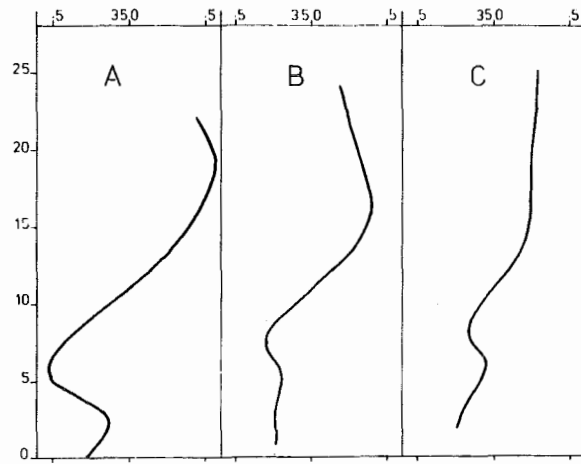


Fig. 14. Different t-S patterns of the Mozambique Channel.

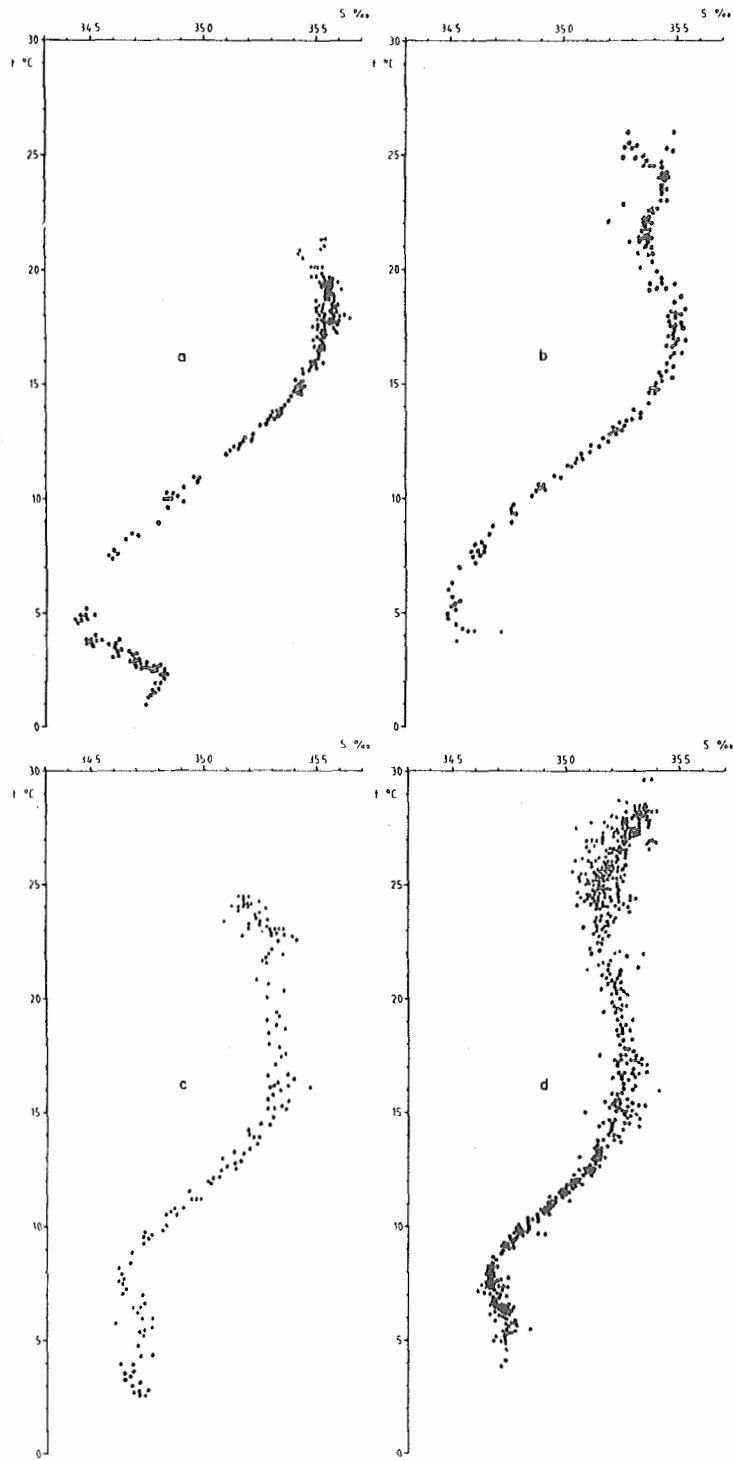


Fig. 15. t-S scattering diagram. a) A structure COMMANDANT ROBERT GIRAUD Jul.-Aug. 1960. b) A structure COMMANDANT ROBERT GIRAUD Oct.-Nov. 1957. c) B structure COMMANDANT ROBERT GIRAUD Jul.-Aug. 1960. d) B structure COMMANDANT ROBERT GIRAUD Oct.-Nov. 1957.

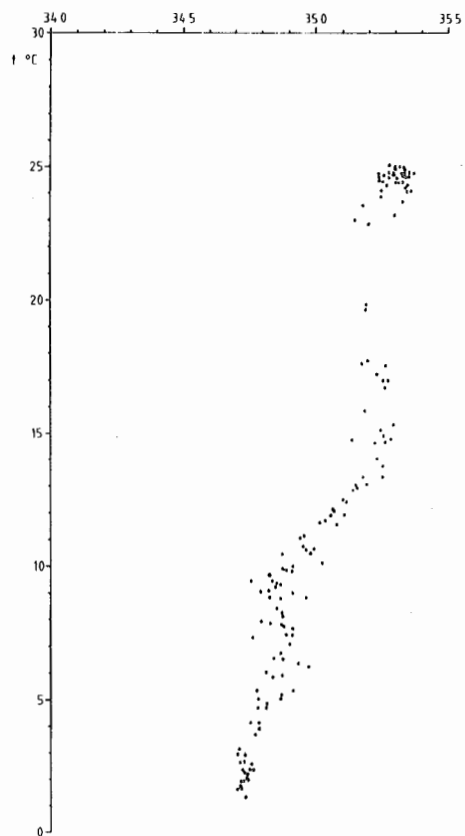


Fig. 16. t-S scattering diagrams from the
COMMANDANT ROBERT GIRAUD Jul.-
Aug. 1960, C-structure.

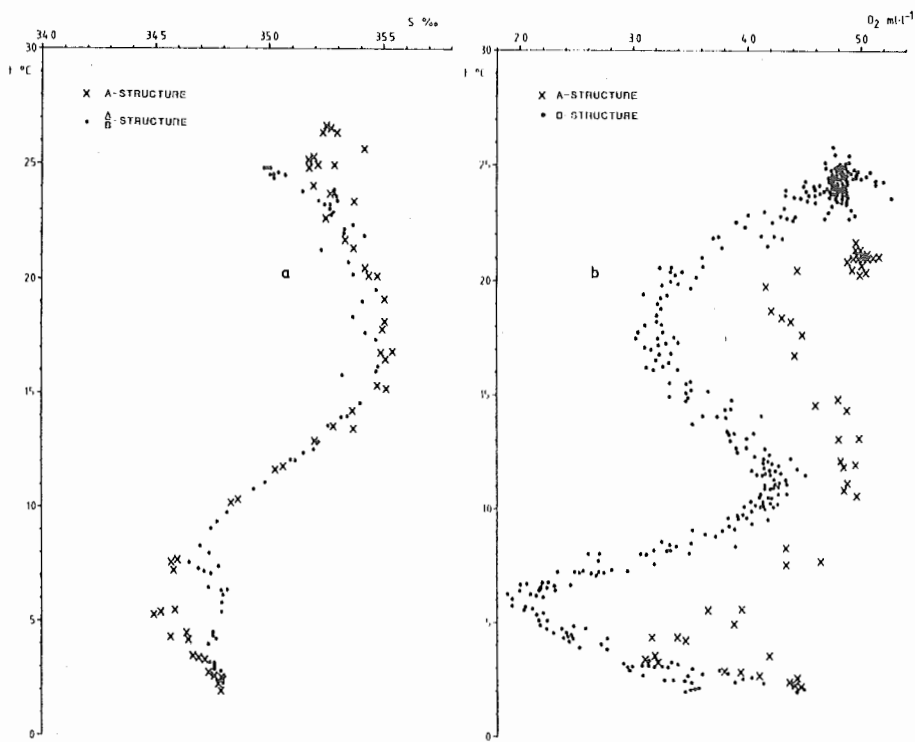


Fig. 17. ALMIRANTE LACERDA 1964. a) t-S diagram,
Apr.-May. b) t-O₂ diagram, Sep.-Oct.

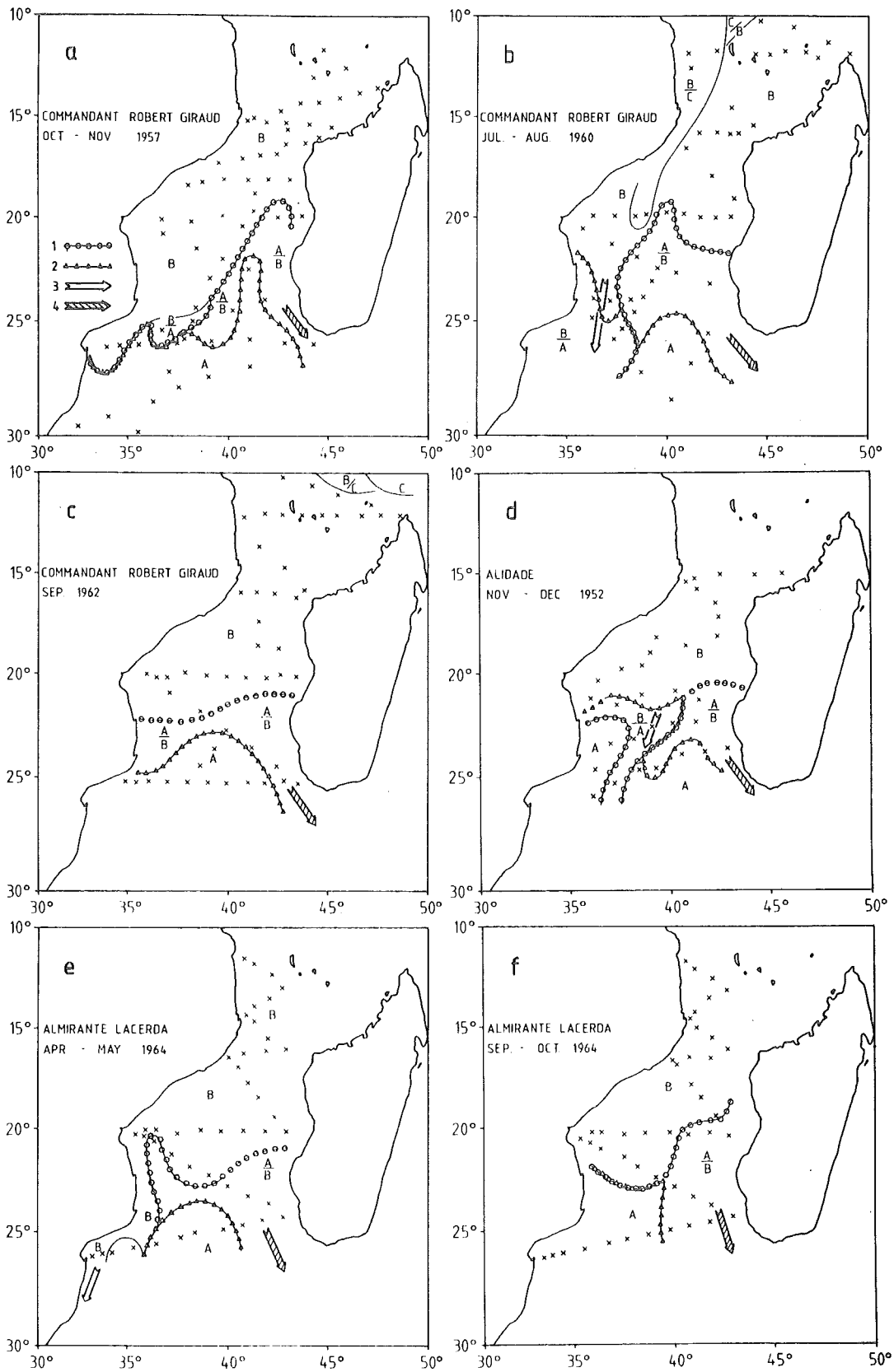


Fig. 18. Distribution of the water mass structures from the six cruises. 1) Borderline between A and B structures - upper layer. 2) Borderline between A and B structures - lower layer. 3) Outflow upper layer. 4) Outflow lower layer.

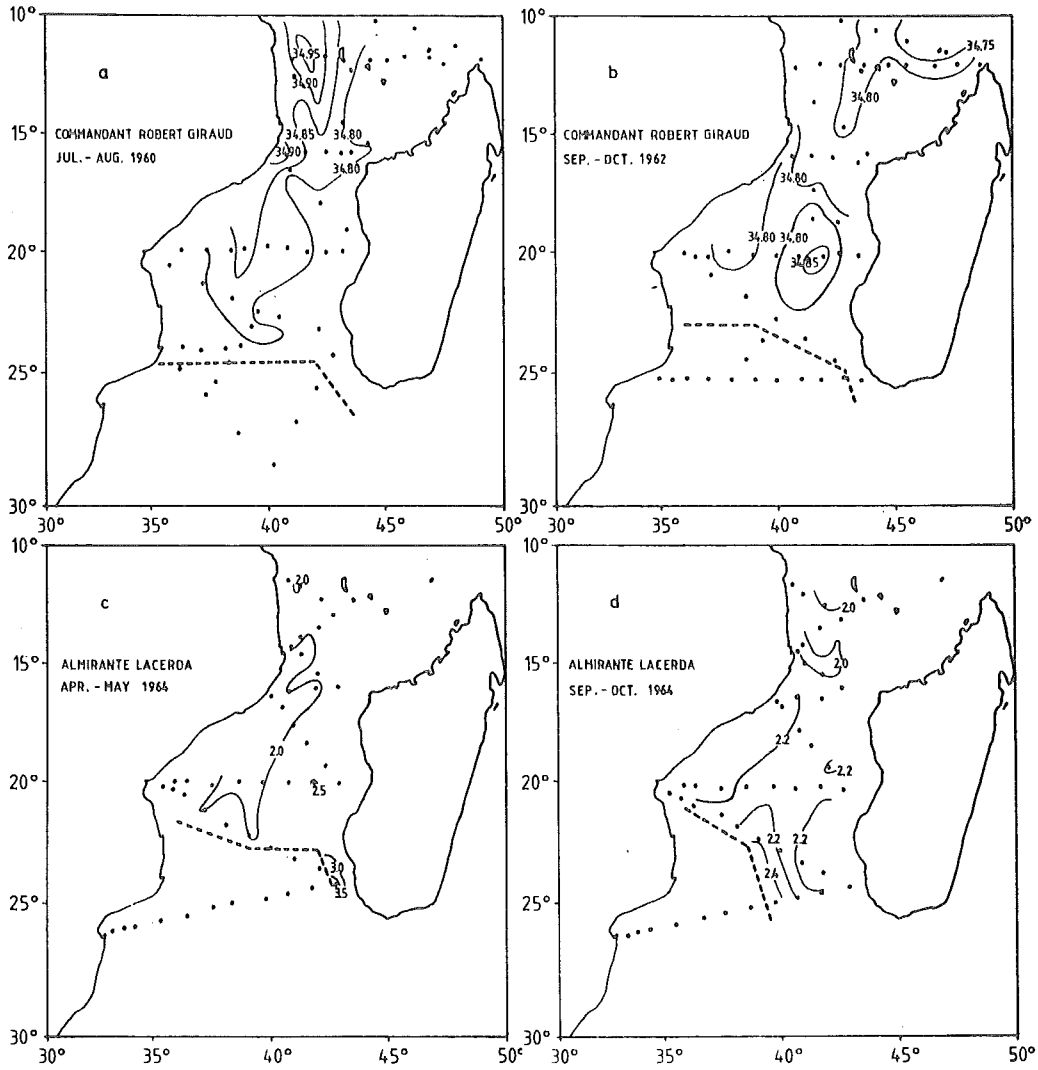


Fig. 19. North Indian Intermediate Water. a, b) Salinity at intermediate salinity maximum. c, d) Oxygen (ml/l) at intermediate salinity maximum. No maximum observed south of heavy dotted line.

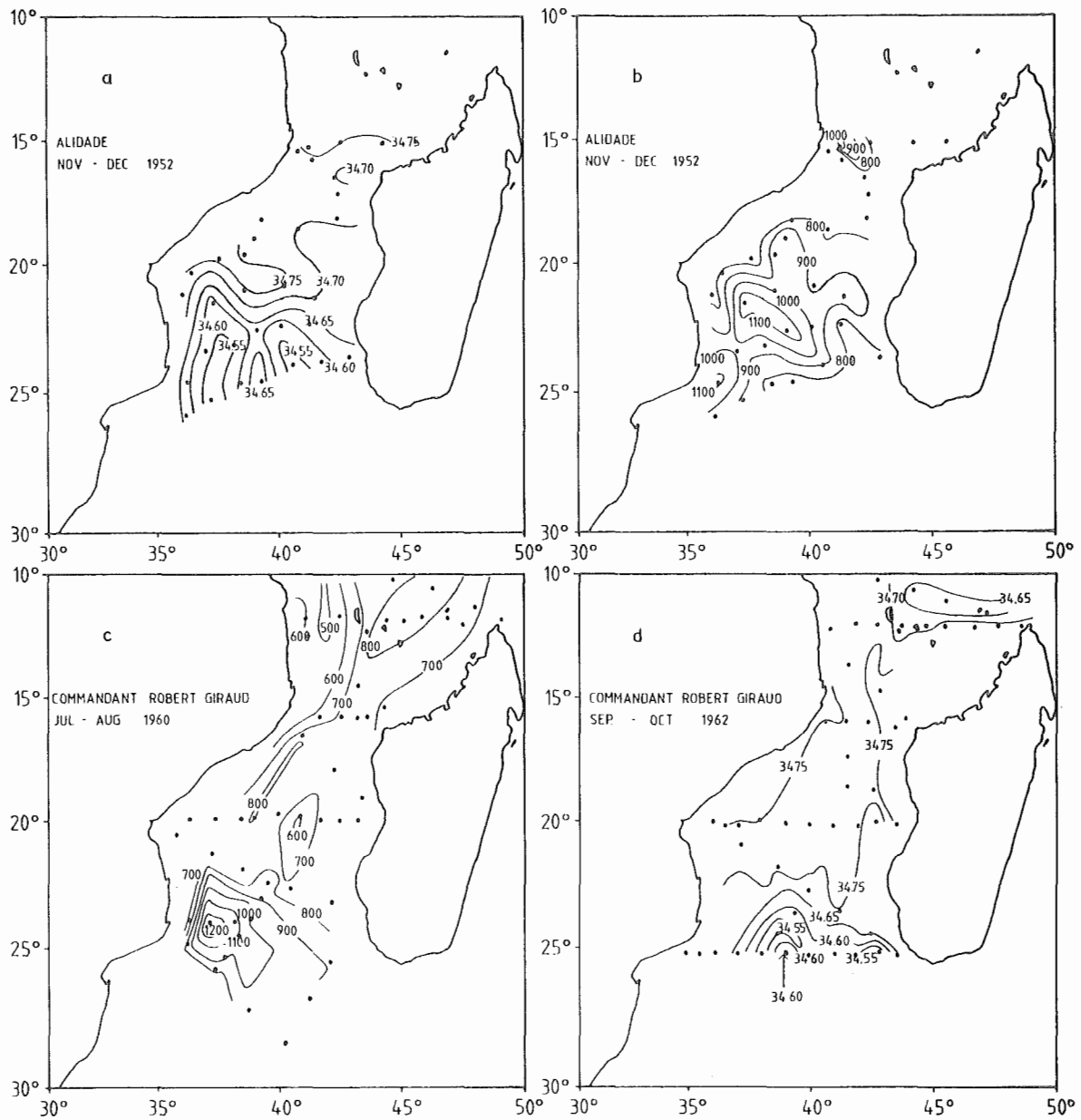


Fig. 20. Antarctic Intermediate Water. a-d) Salinity at intermediate salinity minimum. b-c) Depth of intermediate salinity minimum.

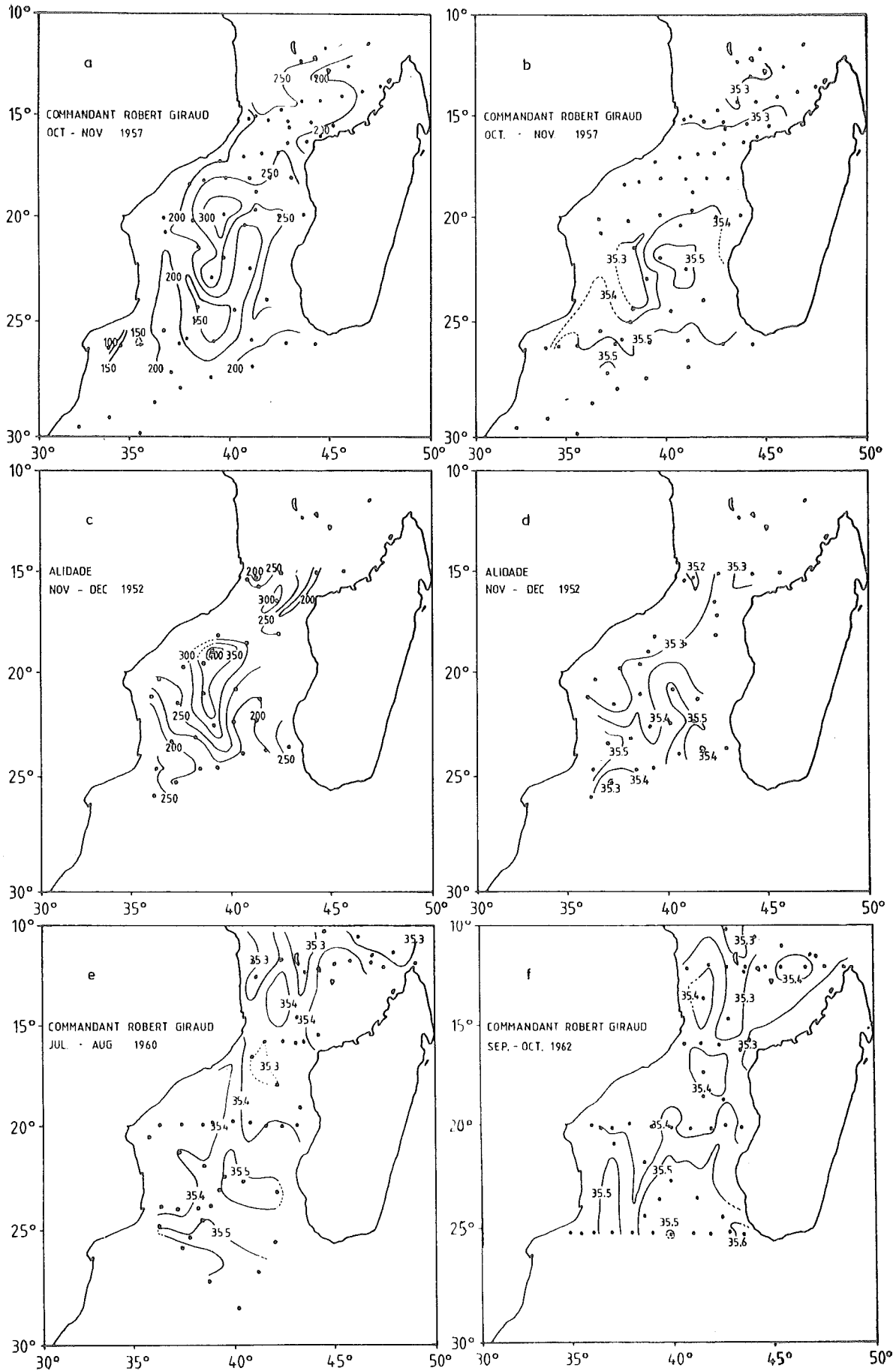


Fig. 21. Subsurface water. a,c) Depth of the subsurface salinity maximum. b,d,e,f) Salinity at subsurface salinity maximum.

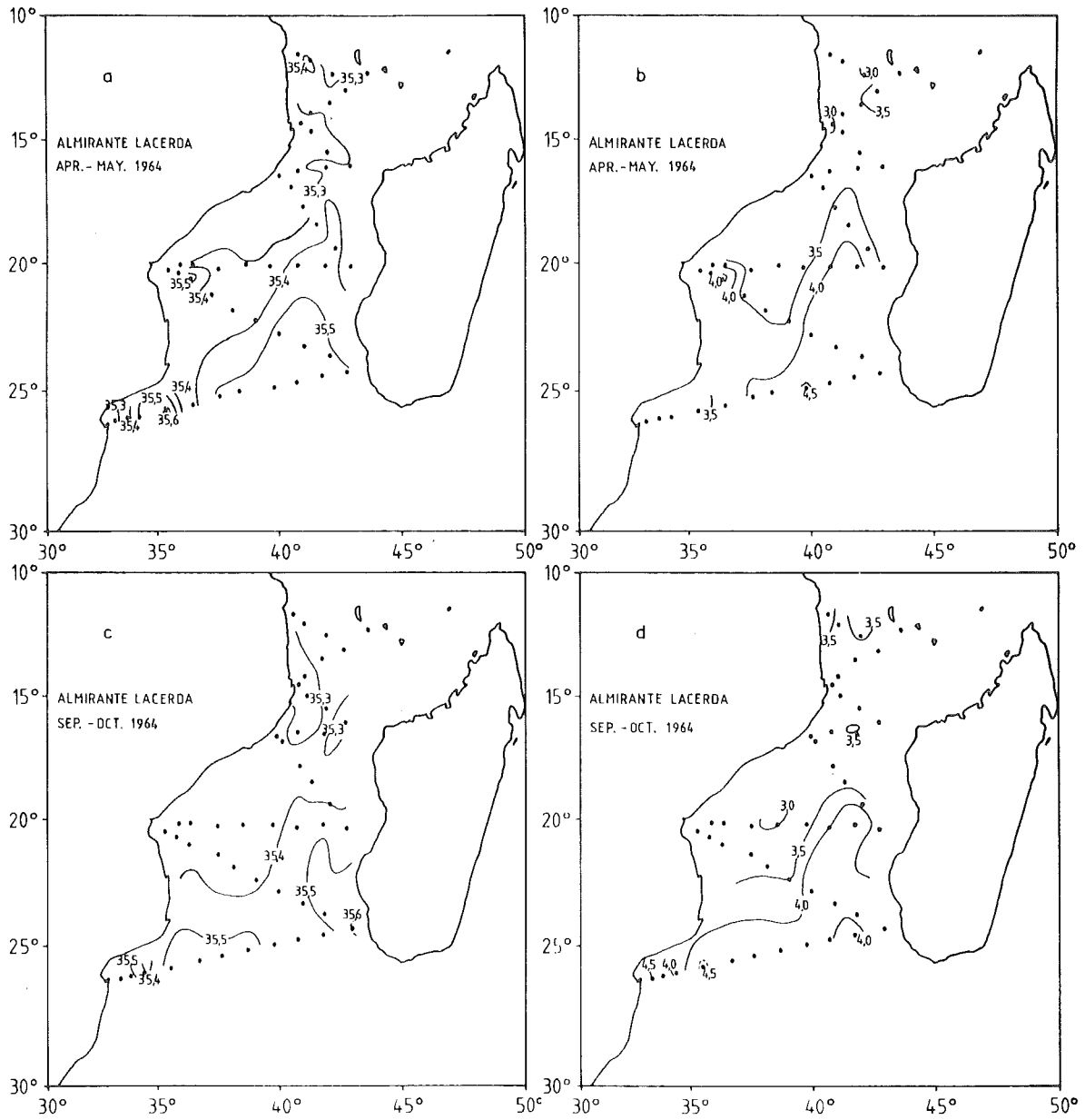


Fig. 22. Subsurface water. a, c) Salinity at the subsurface salinity maximum. b, d) Oxygen (ml/l) at the subsurface salinity maximum.

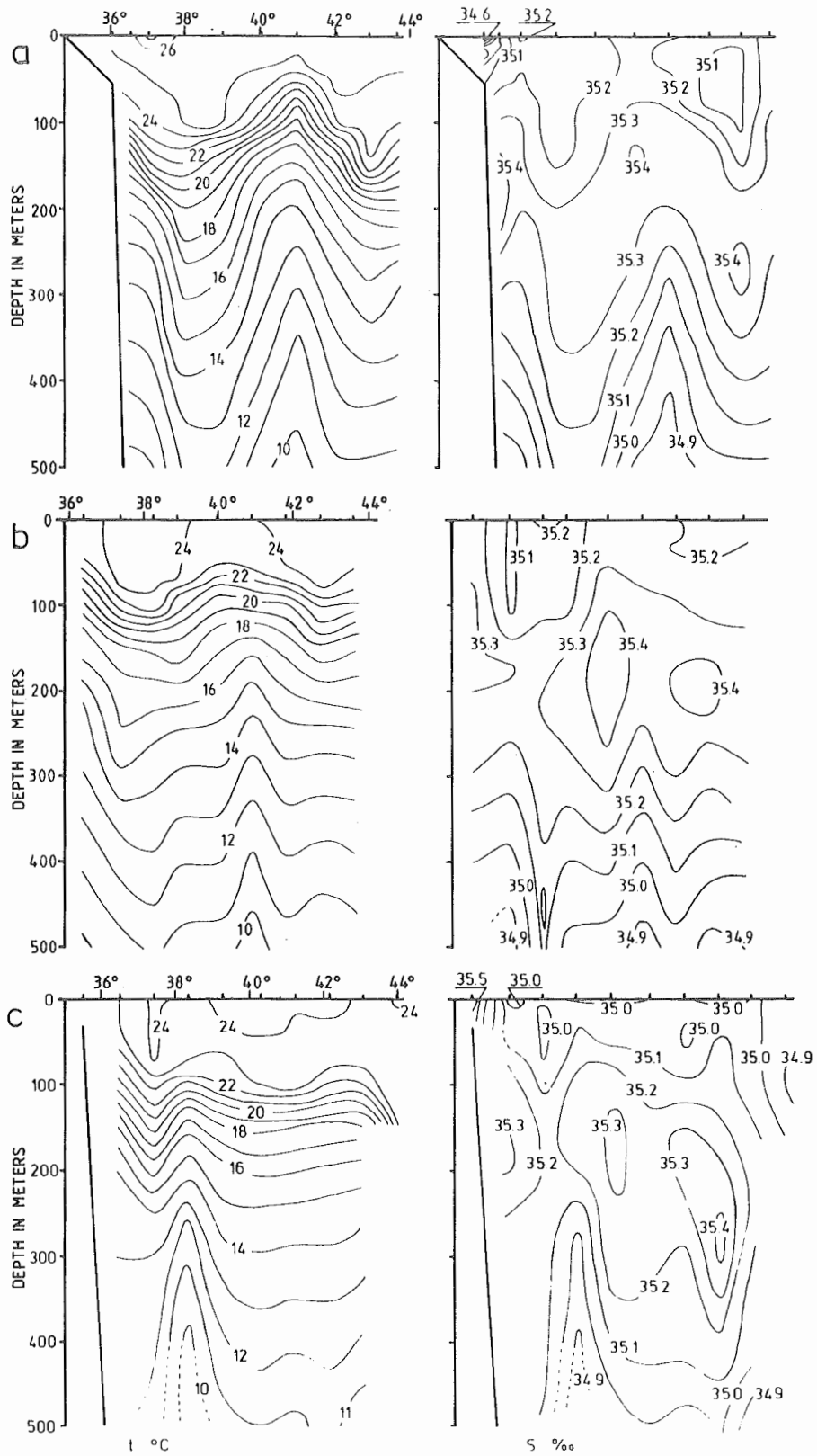


Fig. 23. Hydrographic sections across the Mozambique Channel along 20°S. Mozambique on left side.
a) COMMANDANT ROBERT GIRAUD, 28-30 Sep. 1962.
b) COMMANDANT ROBERT GIRAUD, 27 Jul. - 1 Aug. 1960.
c) ARIEL, 24 Jul. - 5 Aug. 1968.

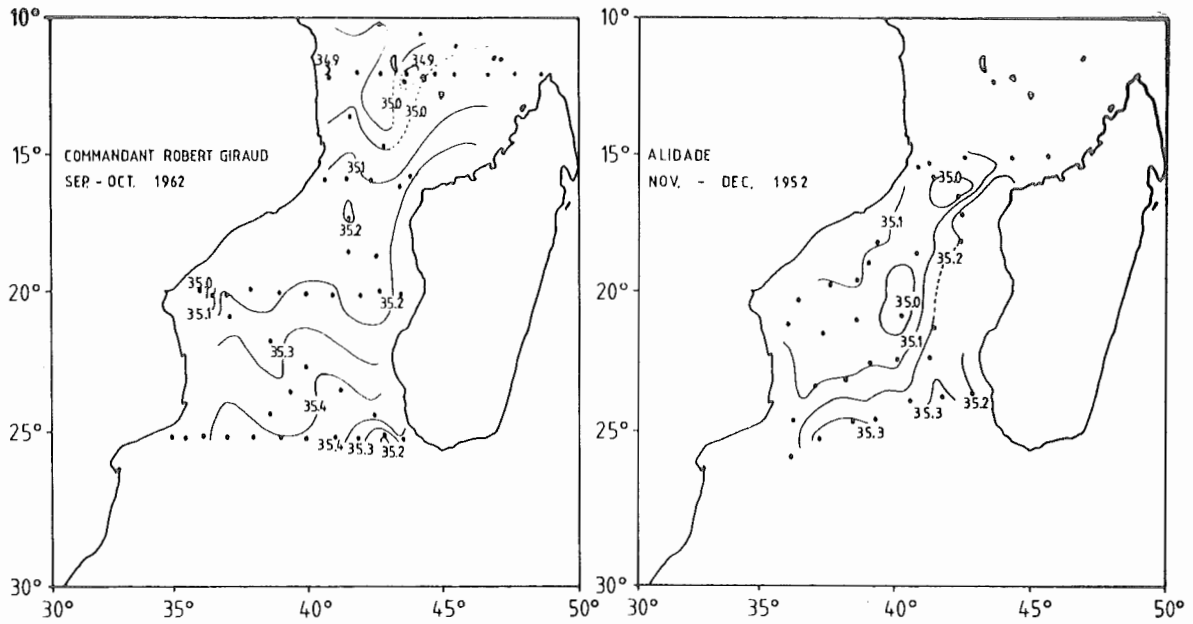


Fig. 24. Surface salinity - COMMANDANT ROBERT GIRAUD 1962 and ALIDADE 1952.

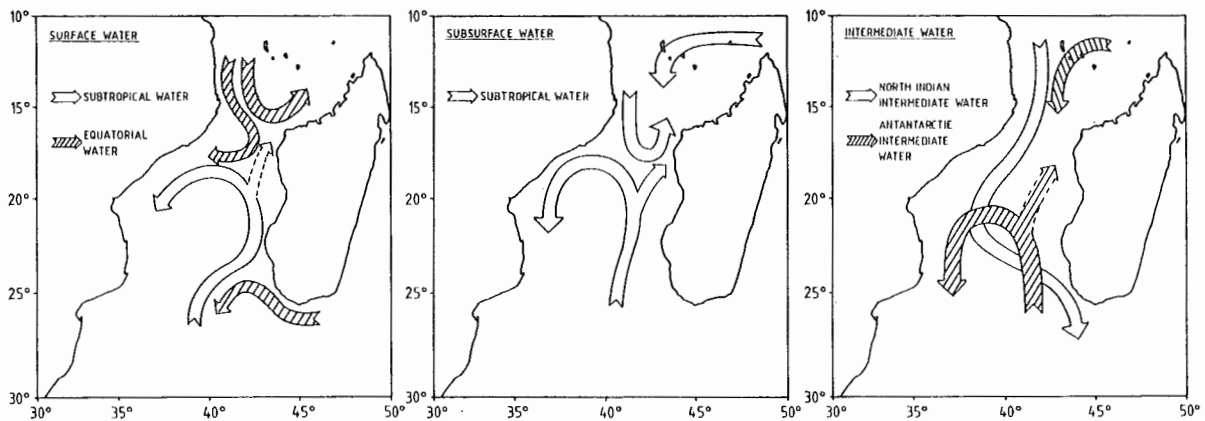


Fig. 25. Tentative paths of propagation for the different water masses of the Mozambique Channel.

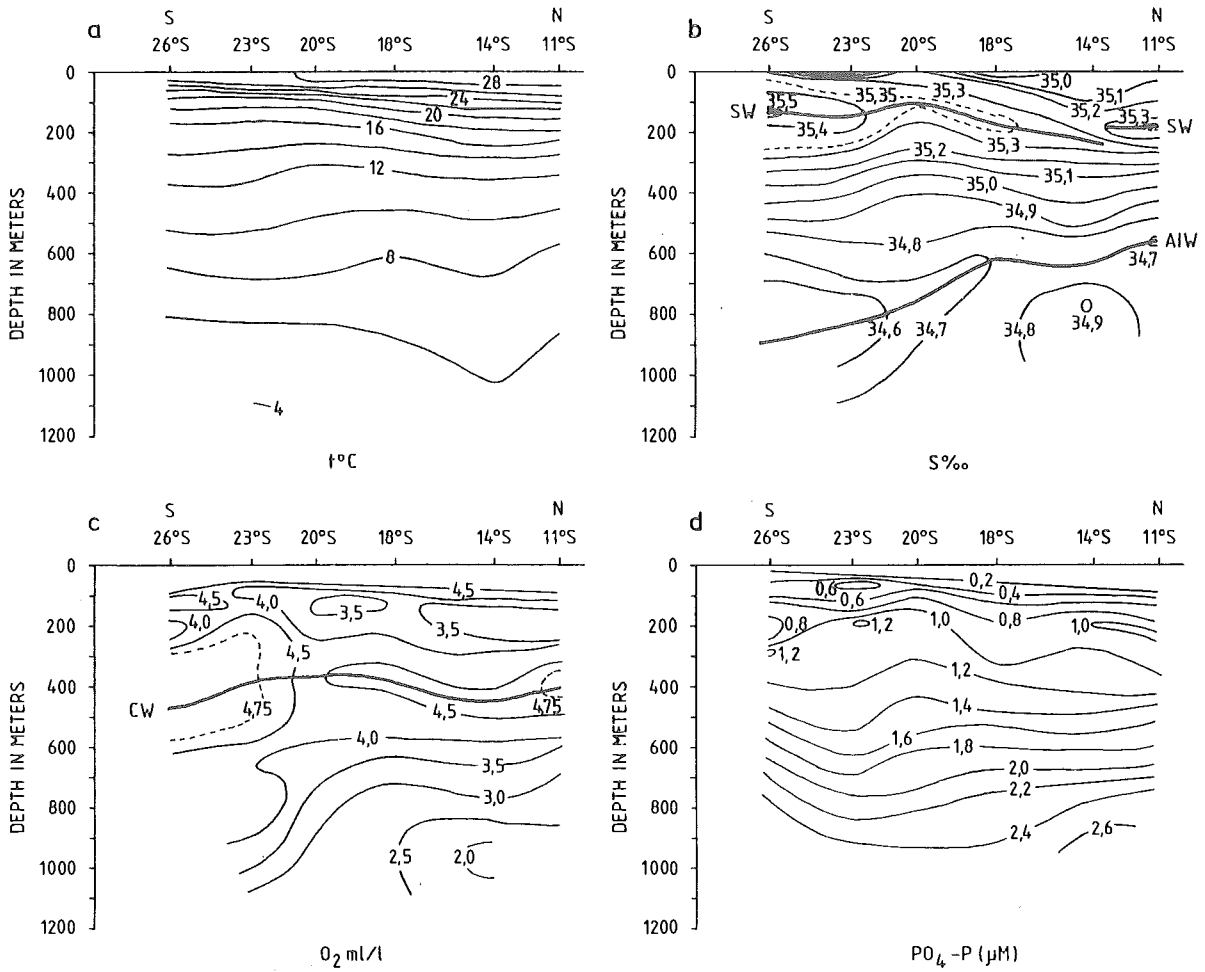


Fig. 26. Longitudinal section along the coast of Mozambique - ERNST HAECKEL, March 1979. SW - Sub-tropical water, AIW - Antarctic Intermediate water, CW - Central water.

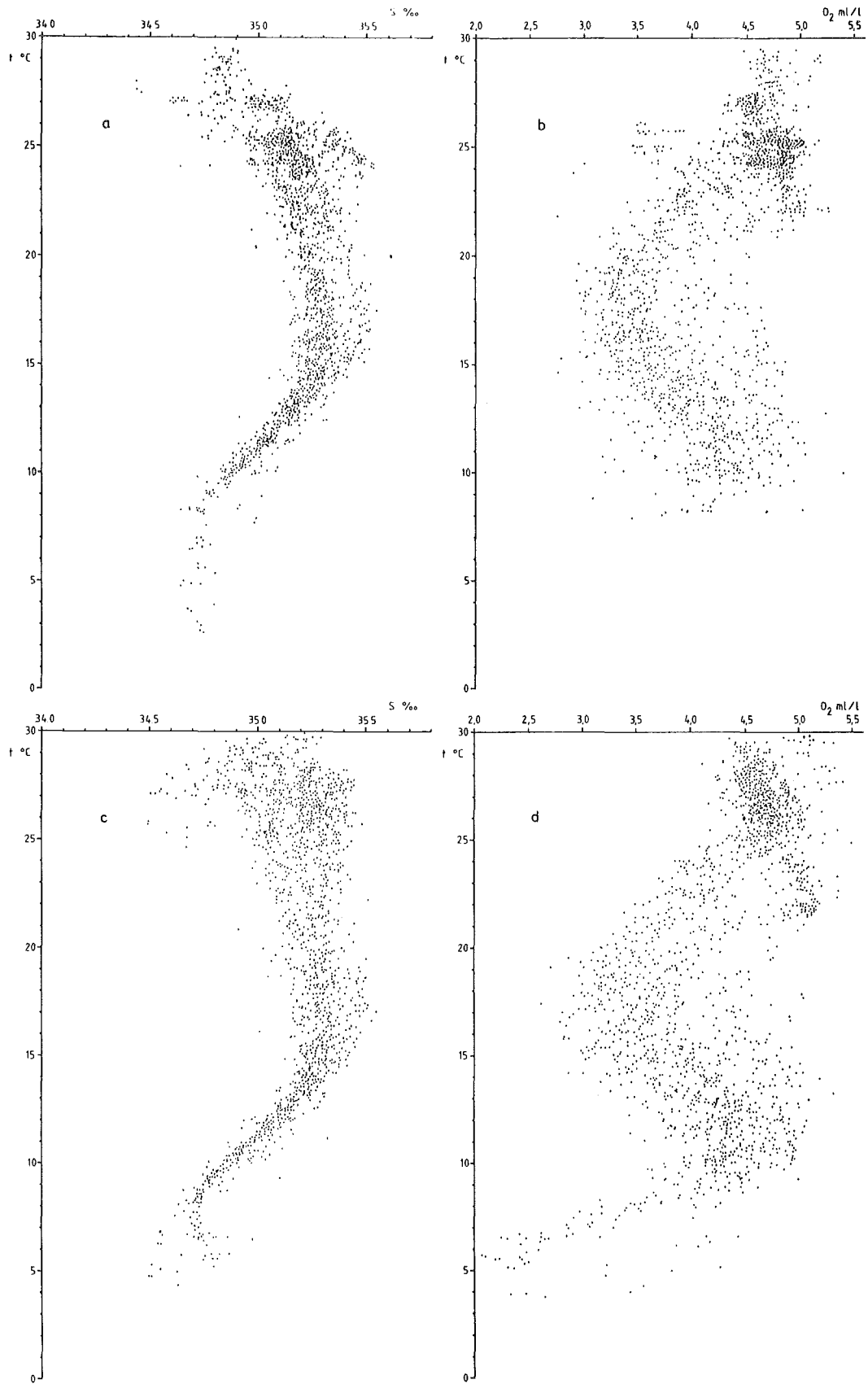


Fig. 27. t - S and t - O_2 for the hydrographic data of Table 1.
a and b) April-September. c and d) October-March.

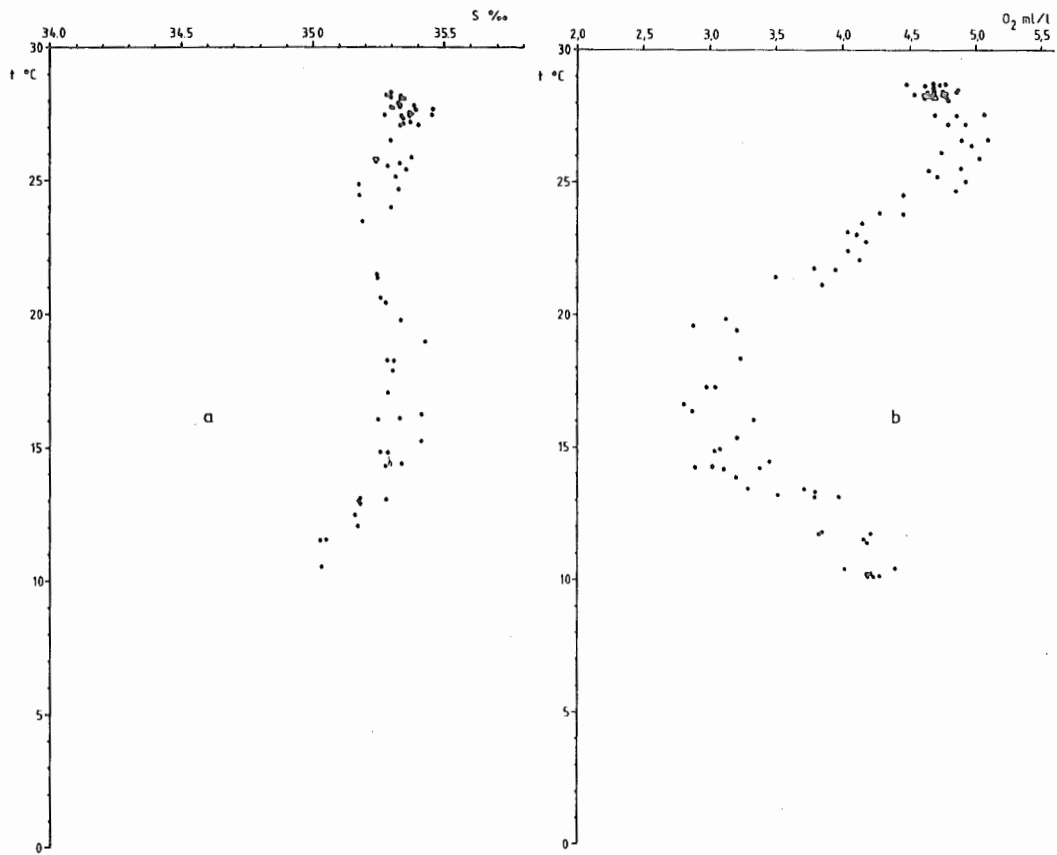


Fig. 28. t-S and t-O₂ diagrams from a section along 21°35'S - December 1978.

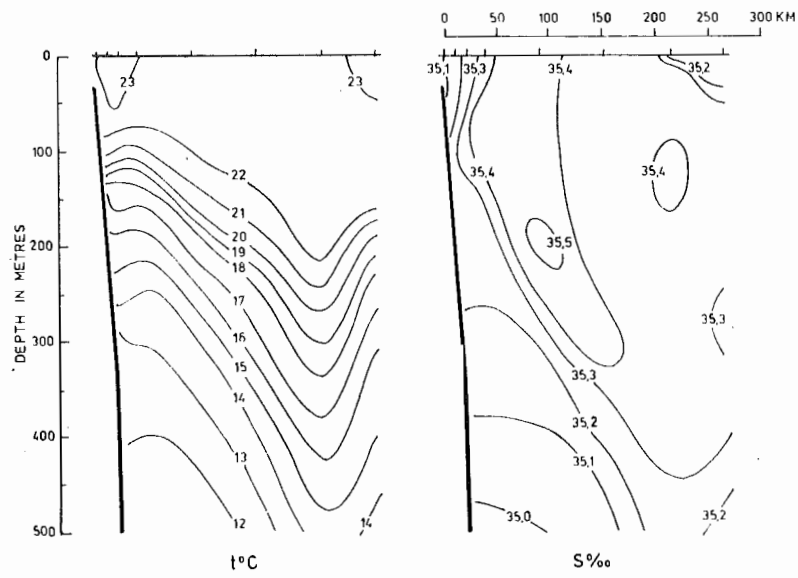


Fig. 29. ERNST HAECKEL - August 1980. Section along 22°20'S.

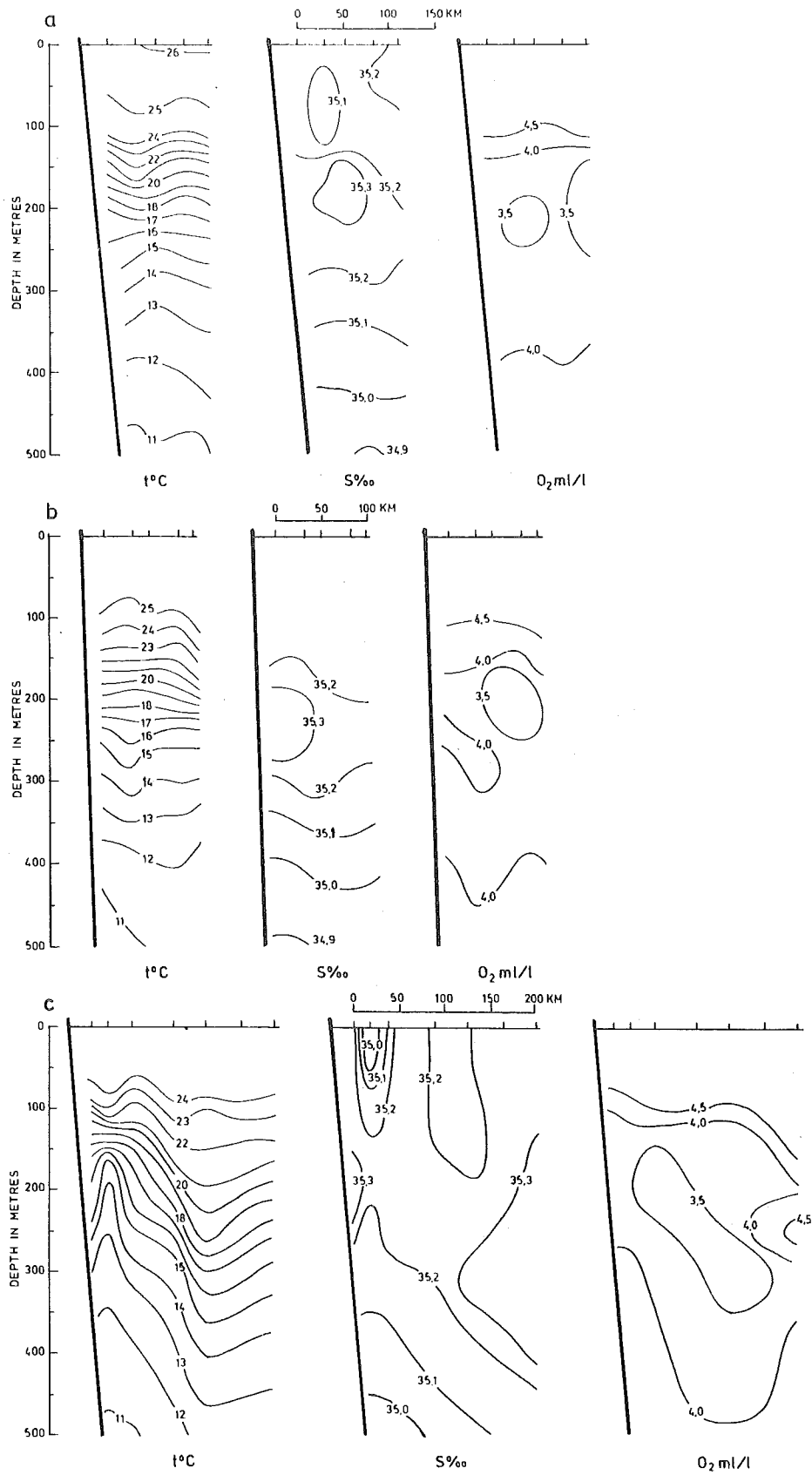


Fig. 30. MYSLITEL - September 1978. Section along
a) 11°S b) 14°S c) 21°30'S.

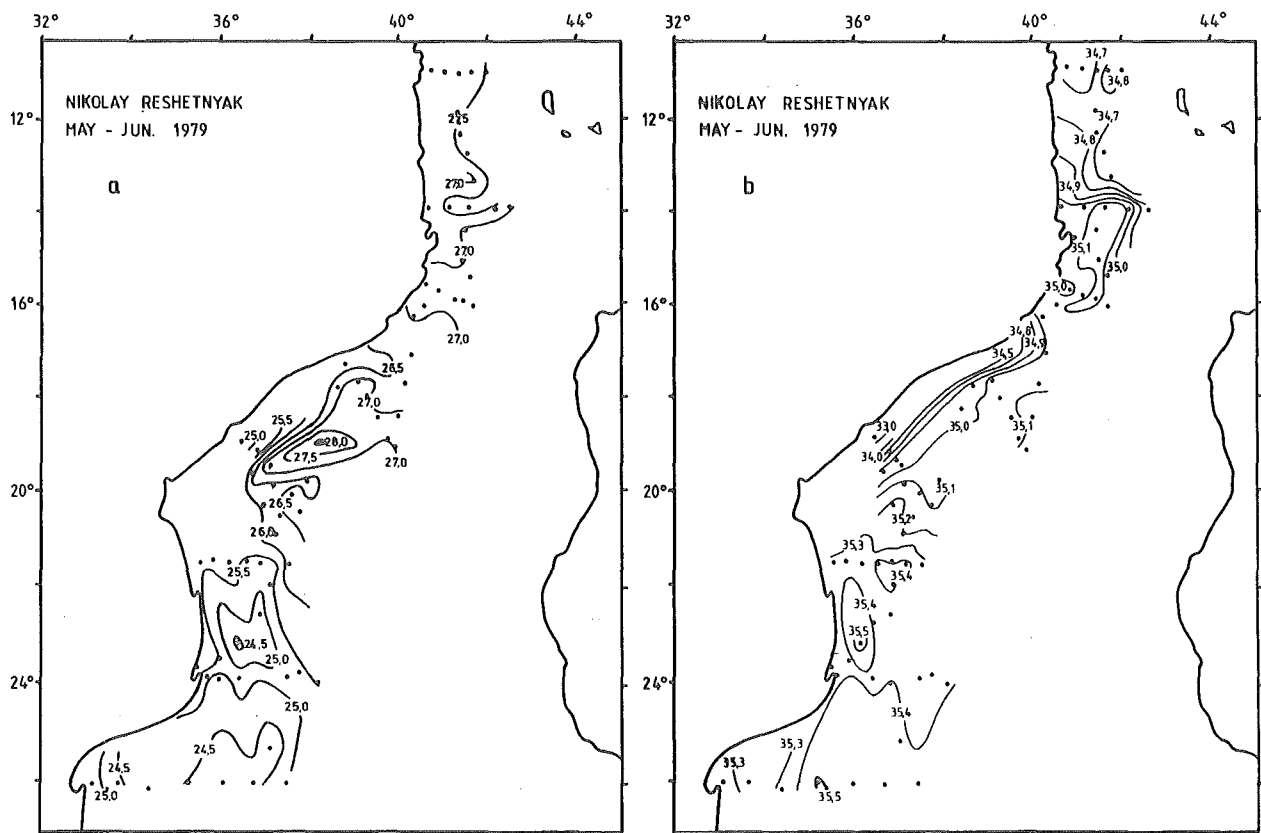


Fig. 31. NIKOLAY RESHETNYAK, May-June 1979.
a) Distribution of surface temperatures.
b) Distribution of surface salinities.

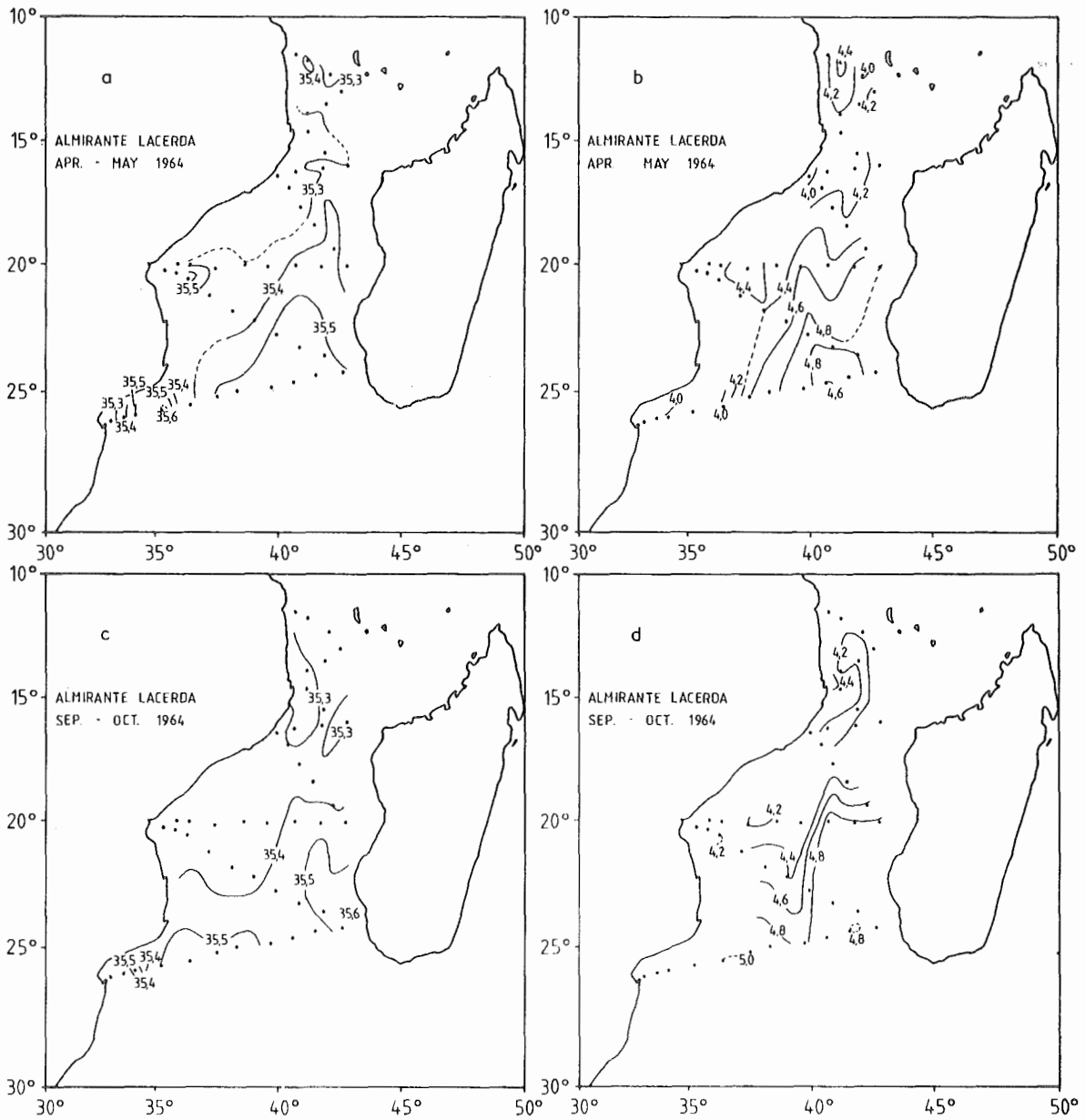


Fig. 32. ALMIRANTE LACERDA - a, c) Salinity at subsurface salinity maximum. b, c) Oxygen at intermediate oxygen maximum.

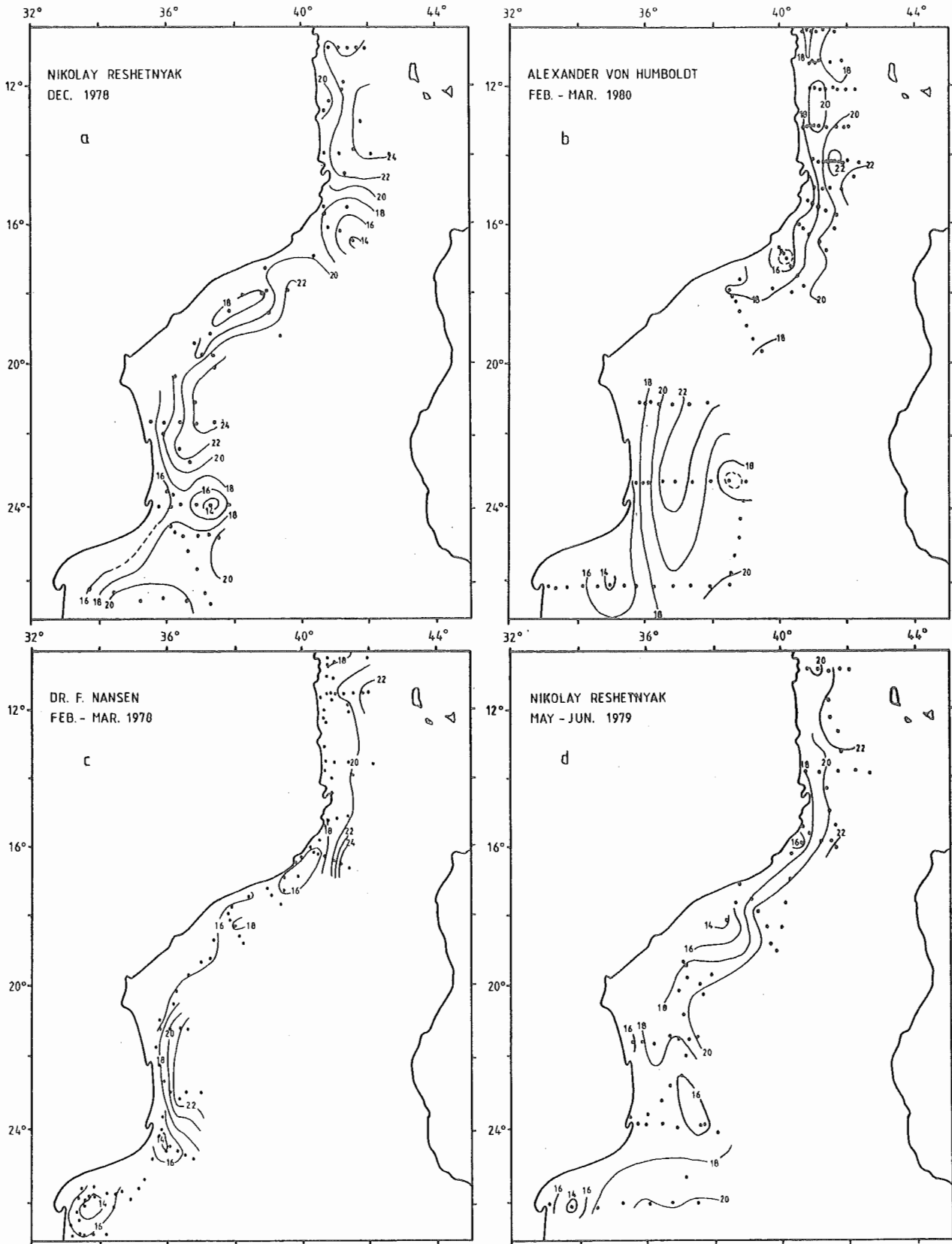


Fig. 33. Distribution of temperatures at 150 m depth.

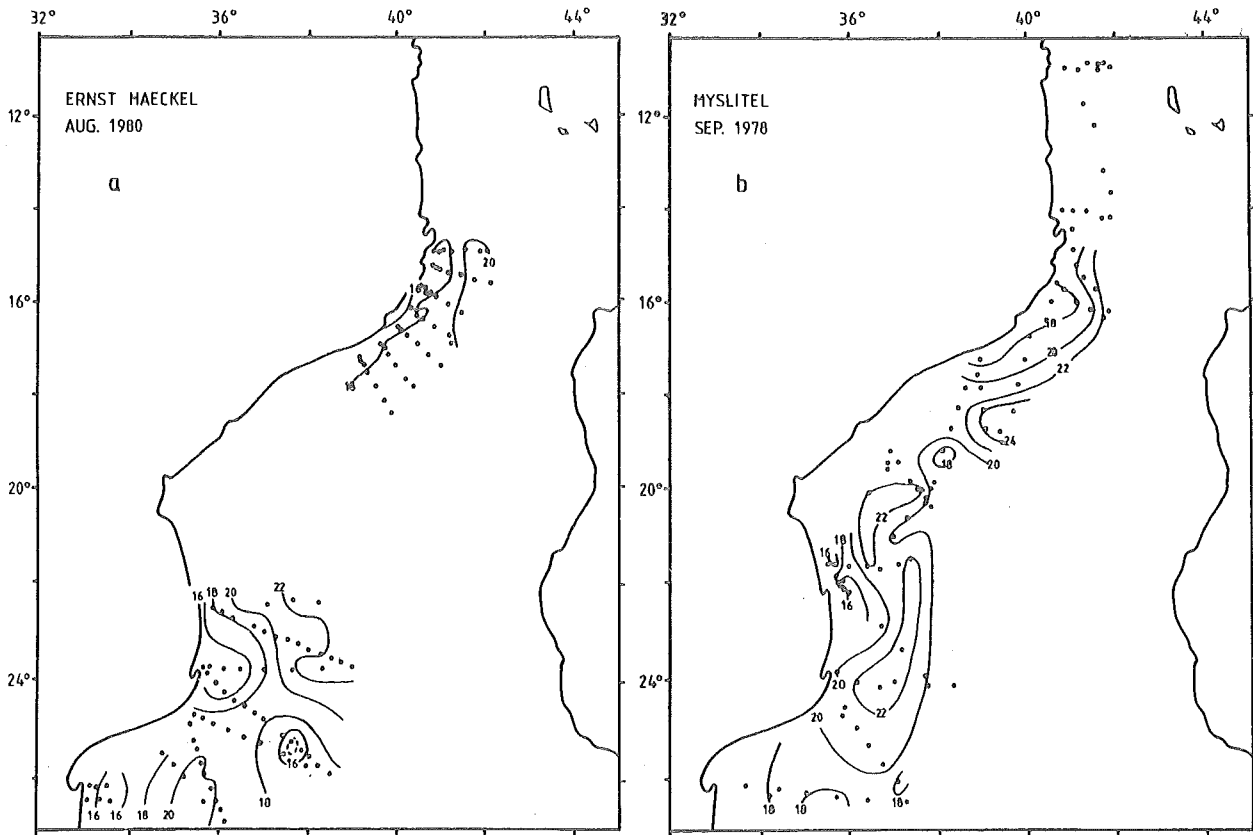


Fig. 34. Distribution of temperatures at 150 m.

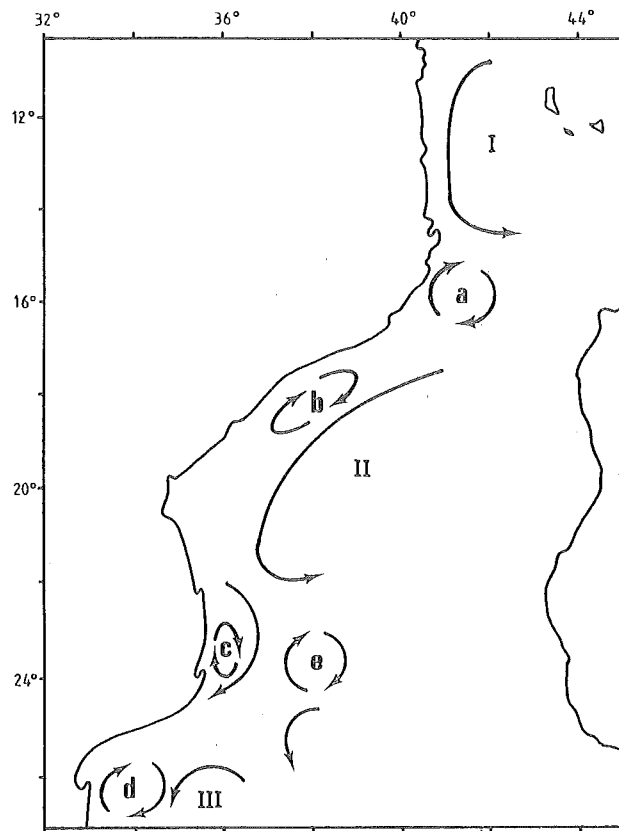


Fig. 35. Dynamic features off the Mozambican coast.

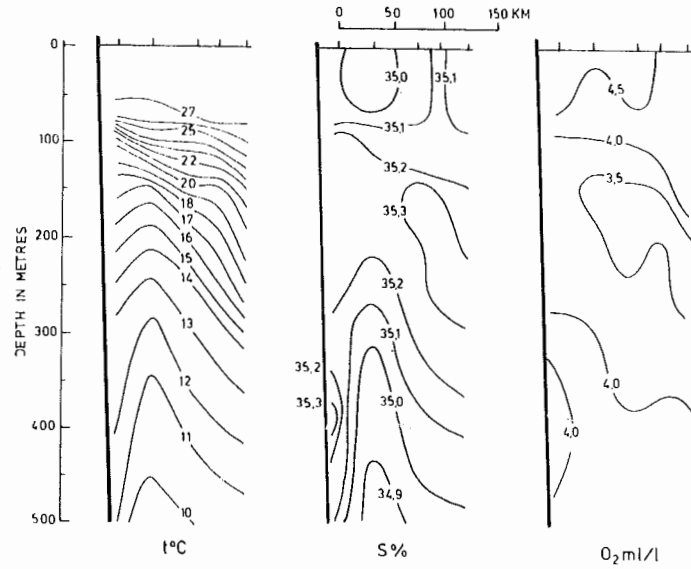


Fig. 36. NIKOLAY RESHETNYAK - June 1979.
Section towards south-east with
mid-latitude of 16°S.

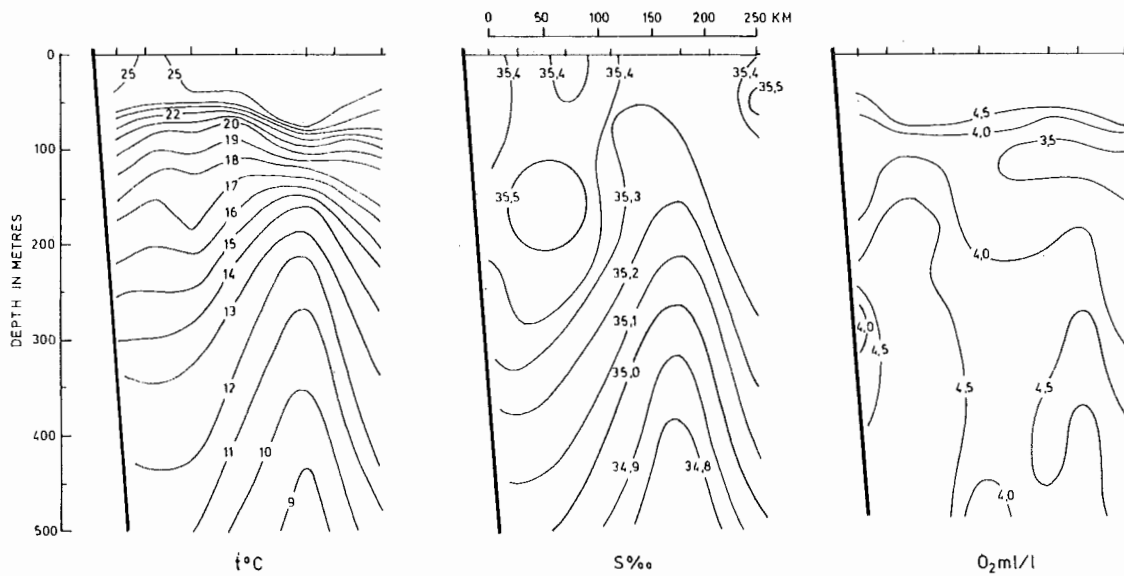


Fig. 37. NIKOLAY RESHETNYAK - May 1979. Section along 24°S.

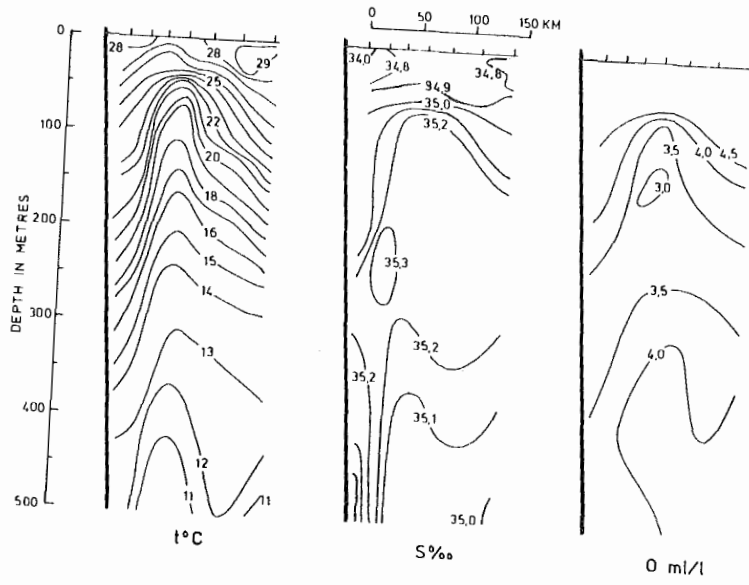


Fig. 38. DR. FRIDTJOF NANSEN - April 1978.
Section from Angoche towards the south-east.

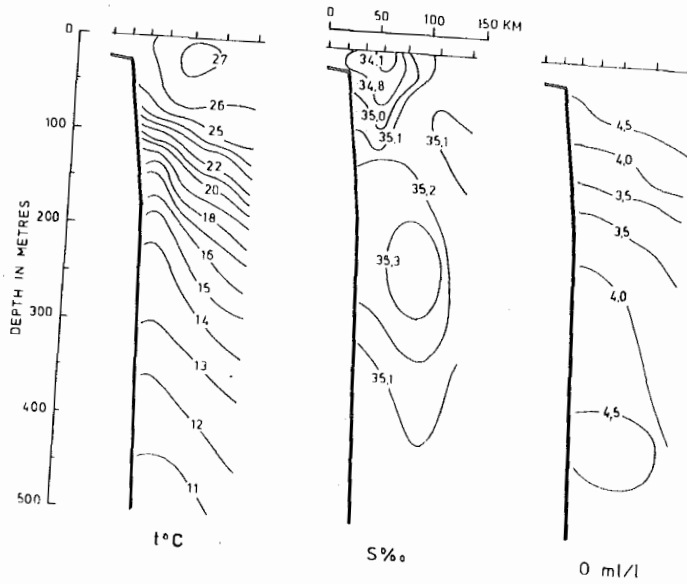


Fig. 39. DR. FRIDTJOF NANSEN - May 1978.
Section along 21° 10' S.

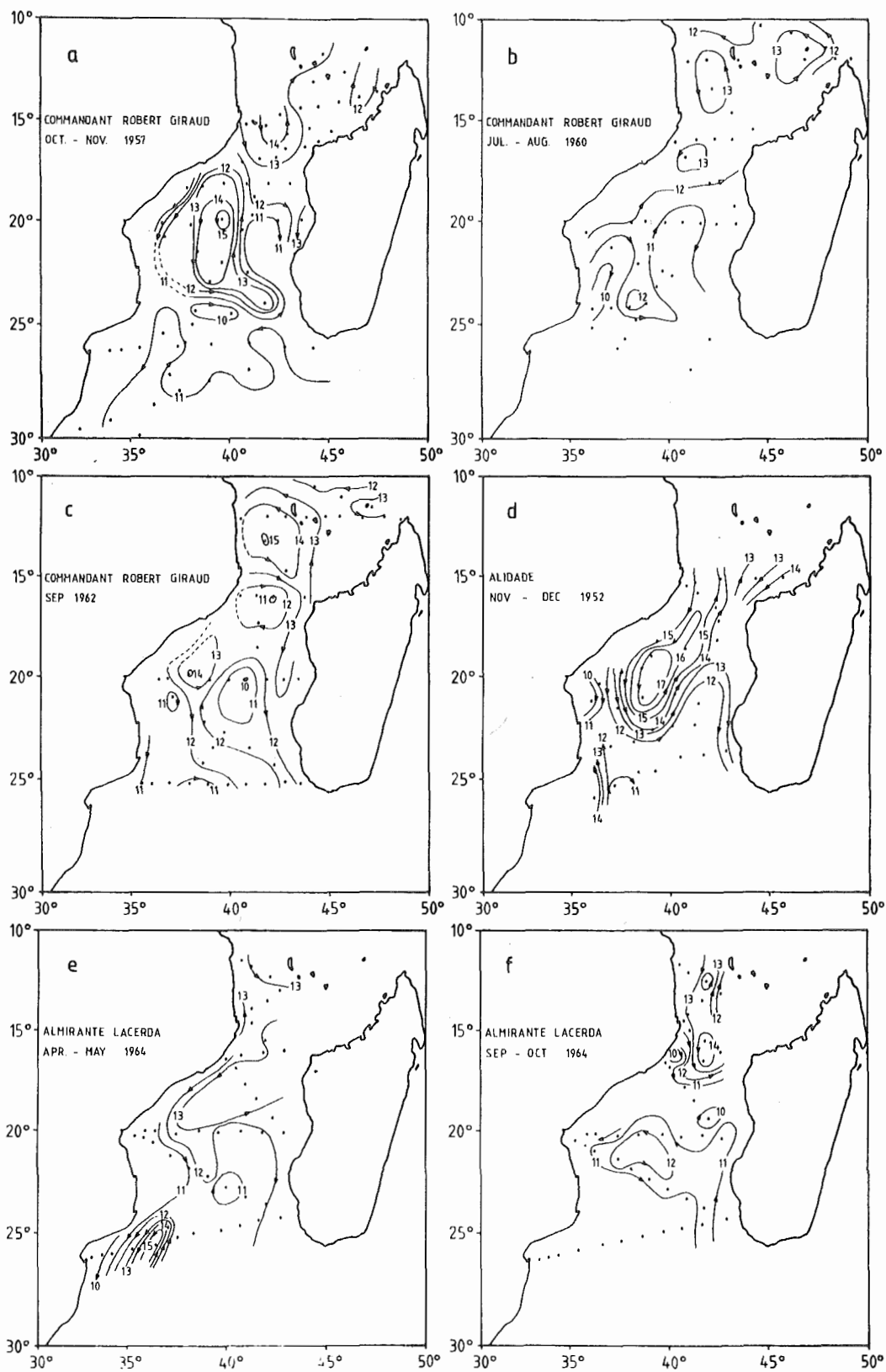


Fig. 40. Dynamic topography (in dyn dm) of the sea surface relative to the 500 decibar level.

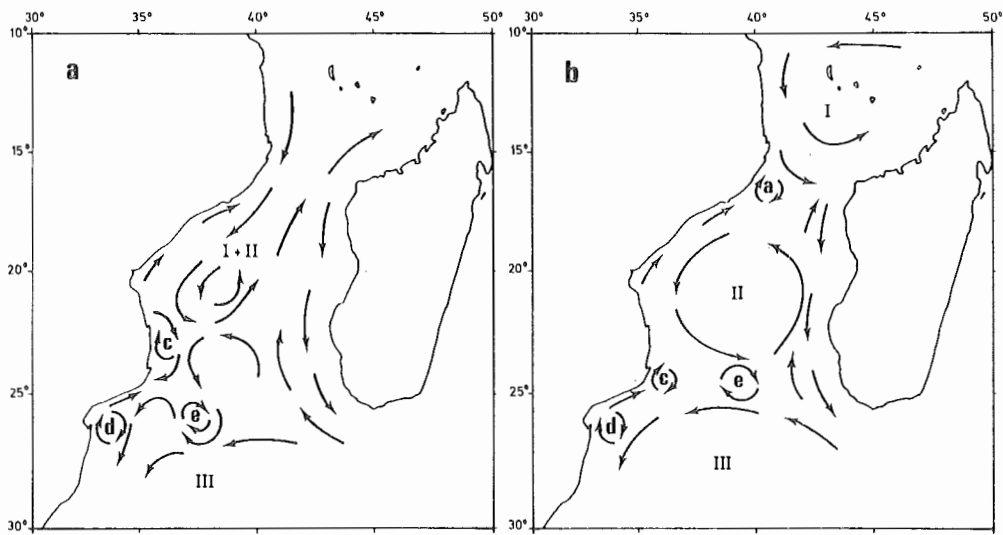


Fig. 41. Tentative circulation patterns in the upper layer of the Mozambique Channel.